

**DESIGN AND TESTING OF A NOVEL INTERVENTION  
CONFIGURATION FOR THE LANE KEEPING SYSTEM  
FOR VEHICLES**

**TAŞITLARA YÖNELİK ŞERİT KORUMA SİSTEMİ İÇİN  
YENİLİKÇİ BİR MÜDAHALE KONFIGÜRASYONUN  
TASARIMI VE SINANMASI**

**MORTEZA DOUSTI**

**ASST. PROF. DR. EMİR KUTLUAY**

**Supervisor**

Submitted to

Graduate School of Science and Engineering of Hacettepe University

as a Partial Fulfillment to the Requirements

for the Award of the Degree of Doctor of Philosophy

in Mechanical Engineering.

January 2023

# **ABSTRACT**

## **DESIGN AND TESTING OF A NOVEL INTERVENTION CONFIGURATION FOR THE LANE KEEPING SYSTEM FOR VEHICLES**

**Morteza DOUSTI**

**Doctor of Philosophy, Department of Mechanical Engineering**

**Supervisor: Asst. Prof. Dr. Emir KUTLUAY**

**January 2023, 80 pages**

This study presents a novel intervention configuration for lane keeping assistance system. The goal of the new configuration is to increase the robustness of the lateral control of the vehicle by utilizing the force potential of three wheels by applying braking torque to one of the rear wheels in coordination with a steering angle input to the front axle. An LQR (Linear-Quadratic Regulator) controller is designed using a single-track vehicle model and then tested in a simulation environment using Simulink and CarMaker software. In order to observe the performance of the system, three test cases were designed in which yaw rate, yaw angle, and lateral error were used as test inputs. The performance of the proposed intervention configuration was compared with only steering and only braking configurations. Test results show that the coordinated steering and brake control configuration provided the best performance with the lowest control input compared to the other two configurations. The new intervention configuration improved the response speed of the lane keeping considerably. The predictive model controller (MPC) was designed to improve the configuration's performance and compared with the LQR performance with the clothoid ramp experiment. The new configuration with MPC has succeeded in displaying high-level performance.

**Keywords:** Lane Keeping Assistance, Yaw, Intervention configuration, Coordinated steering & braking intervention, LQR, MPC, Step Response

# ÖZET

## TAŞITLARA YÖNELİK ŞERİT KORUMA SİSTEMİ İÇİN YENİLİKÇİ BİR MÜDAHALE KONFIGÜRASYONUN TASARIMI VE SINANMASI

**Morteza DOUSTI**

**Doktora, Makina Mühendisliği Bölümü**

**Danışmanı: Asst. Prof. Dr. Emir KUTLUAY**

**Ocak 2023, 80 sayfa**

Bu çalışmada şerit takip sistemleri için yenilikçi bir müdahale konfigürasyonu sunulmuştur. Amacı taşıtın yanal kontrol gürbüzlüğünü arttırmak olan bu yeni konfigürasyon, ön aksa verilen direksiyon açısı ile eşgüdümlü olmak üzere taşıtın arka tekerleklerinden birine uygulanan frenleme torku ile üç tekerleğin kuvvet potansiyelinden faydalanmaktadır. Bunun için tek izli taşıt modeli kullanılarak bir Doğrusal Karesel Regülatör (LQR) kontrolcüsü tasarlanmış, Simulink ve CarMaker programları kullanılarak simülasyon ortamında test edilmiştir. Sistemin performansını gözlemek amacıyla savrulma hızı, savrulma açısı ve yanal mesafe değişkenleri test girdisi olarak kullanılmıştır. Geliştirilen müdahale konfigürasyonunun performansı yalnızca direksiyon ve yalnızca fren konfigürasyonlarıyla karşılaştırılmıştır. Test sonuçlarına göre, direksiyon ve fren kontrol konfigürasyonu en düşük kontrol girdisini vermeyi başarmış, diğer iki konfigürasyona kıyasla en yüksek performansı göstermiştir. Bu yeni konfigürasyon, şerit takip sisteminin tepki süresinde önemli ölçüde geliştirme sağlamaktadır. Konfigürasyonun performansını arttırmak için öngörücü model kontrolcüsü (MPC) tasarlanmıştır ve klotoyid rampa deneyinde LQR performansı ile kıyaslanmıştır. MPC ile yeni konfigürasyon üst düzey performans sergilemeyi başarmıştır.

**Anahtar Kelimeler:** Şerit takip sistemi, Savrulma, Müdahale konfigürasyonu, Eşgüdümlü direksiyon ve fren müdahalesi, LQR, MPC, basamak cevabı

## ACKNOWLEDGEMENT

First, I would like to express my gratitude and appreciation to my supervisor Assit. Prof. Dr. Emir Kutluay; without his continuous support and help, this thesis would not have been possible. I also would like to say special thank you to Prof. Dr. Mesut Düzgün, and Assoc. Prof. Dr. A. Ufuk Şahin for their support and encouragement throughout the process.

I also would like to say that I enjoyed the time when I was working at the Hacettepe SensTech Research Lab, and it was a great pleasure for me to work with so many friendly people, and I would like to thank you all. I learned a lot from you.

Finally, I owe my most important acknowledgments to my family, whose love and dedication carried me through this thesis project.

# CONTENTS

ABSTRACT .....	i
ÖZET .....	ii
Acknowledgement.....	iii
CONTENTS .....	iv
FIGURES .....	vi
TABLES.....	viii
Nomenclature .....	ix
1. Introduction.....	1
1.1. Literature Survey.....	1
1.2. Safety Overview .....	1
1.3. Market Research.....	2
1.4. Lane Departure Warning System .....	3
1.5. Lane Keeping Assistance System .....	3
1.6. Unintended Lane Departure Problem.....	4
1.7. Intervention Configurations .....	5
1.8. Control Methods.....	8
1.9. Conclusion.....	11
2. Theoretical Background .....	13
2.1. Intervention Configuration.....	13
2.2. Vehicle Model .....	13
2.3. Road Model.....	16
2.4. Controller Design .....	16
2.4.1. Linearized vehicle model .....	16
2.4.2. Linear Quadratic Regulator .....	19
2.4.3. Model Predictive Control .....	23
2.5. Conclusion.....	24
3. Simulation Experiment Design .....	25
3.1. Step Response Maneuver .....	25

3.2. Ramp Response Maneuver .....	30
3.3. Conclusion .....	30
4. RESULTS AND DISCUSSION .....	31
4.1. Intervention Configurations Performance .....	31
4.2. Controllers Performance .....	39
4.3. Ramp Response Maneuver (Clothoid Spiral) .....	45
4.4. Conclusion .....	50
5. Conclusion .....	52
6. References.....	54
APPENDICES .....	59
Appendix 1 – LQR Design .....	59
Appendix 2 – MPC Design.....	61
EK 4 - Tezden Türetilmiş Yayınlar .....	78
EK 5 - Tezden Türetilmiş Bildiriler.....	79
EK 6 - Tez Çalışması Orjinallik Raporu.....	80
CURRICULUM VITAE.....	81

## FIGURES

Figure 1. ULD problem schematic .....	5
Figure 2. Rear-axle brake pressure build-up of CarMaker model (Response time = 0.005[s] , Build-up time = 0.08[s]).....	14
Figure 3. Step response test of the brake pedal .....	15
Figure 4. Sine sweep test of the steering system.....	15
Figure 5. Simple two-track Lateral Vehicle Model.....	16
Figure 6. One-track Vehicle Model.....	17
Figure 7. General MPC scheme at k'th step.....	23
Figure 8. A typical step response diagram .....	27
Figure 9. The constant radius of curvature maneuver schematic .....	28
Figure 10. The constant radius of curvature maneuver in CarMaker: <b>a)</b> Left, <b>b)</b> Right .	28
Figure 11. Angle step maneuver schematic .....	29
Figure 12. Angle step maneuver in CarMaker: <b>a)</b> Left, <b>b)</b> Right.....	29
Figure 13. Lateral distance step maneuver schematic .....	29
Figure 14. Lateral distance step maneuver schematic in CarMaker .....	30
Figure 15. Constant Curvature Step Test, Intervention configurations error.....	33
Figure 16. Constant Curvature Step Test, Intervention configurations, controller input	33
Figure 17. Angle Step Test, Intervention configurations, controller input .....	34
Figure 18. Angle Step Test, Intervention configurations error .....	35
Figure 19. Lateral Distance Step Test, Control Inputs, and performances .....	38
Figure 20. Constant Curvature Step Test of LQR and MPC controllers, Intervention configurations error .....	40
Figure 21. Constant Curvature Step Test of LQR and MPC controllers, control input ..	40
Figure 22. Constant Curvature Step Test of LQR and MPC controllers, velocities, and acceleration.....	41
Figure 23. Angle Step Test of LQR and MPC controllers, controller input .....	42
Figure 24. Angle Step Test of LQR and MPC controllers, yaw and lateral distance error .....	42
Figure 25. Lateral Distance Step Test of LQR and MPC controllers, Control Inputs, and performances .....	44

Figure 26. Bird's eye view of the clothoid spiral ramp experiment path .....	45
Figure 27. The clothoid spiral ramp experiment path schematic in CarMaker .....	45
Figure 28. Road and vehicle path, LQR and MPC Lane tracking .....	46
Figure 29. Lateral Distance and Yaw Angle error, Lane ID.....	47
Figure 30. Yaw Rate error distribution during Lane Tracking .....	47
Figure 31. Steering Angle input, degree of road curvature, controller comparison .....	48
Figure 32. Torque input for Rear Left (RL) and Rear Right (RR) .....	48
Figure 33. Longitudinal ( $V_x$ ) and Lateral ( $V_y$ ) velocity, Lateral Acceleration ( $a_y$ ) .....	49
Figure 34. Tire Force Usage, Left.....	49
Figure 35. Tire Force Usage, Right .....	50



## TABLES

Table 1. Maneuvers used in experiments .....	26
Table 2. Constant Curvature Step Test, Controller input performance ( $\rho=400\text{m}$ , $\theta=90^\circ$ , $U=19.45\text{ m/s}$ ).....	32
Table 3. Constant Curvature Step Test, Error, and model output performance ( $\rho=400\text{m}$ , $\theta=90^\circ$ , $U=19.45\text{ m/s}$ ).....	32
Table 4. Angle Step Test, Controller input performance ( $U=19.45\text{ m/s}$ ).....	35
Table 5. Angle Step Test, Error, and model output performance ( $U=19.45\text{ m/s}$ ).....	36
Table 6. Lateral Distance Step Test, Controller input performance ( $U=19.45\text{ m/s}$ ).....	37
Table 7. Lateral Distance Step Test, Error, and model output performance ( $U=19.45\text{ m/s}$ ) .....	37
Table 8. Constant Curvature Step Test of LQR and MPC controllers, Controller input performance ( $\rho=400\text{m}$ , $\theta=90^\circ$ , $U=19.45\text{ m/s}$ ).....	39
Table 9. Constant Curvature Step Test of LQR and MPC controllers, Error, and model output performance ( $\rho=400\text{m}$ , $\theta=90^\circ$ , $U=19.45\text{ m/s}$ ).....	39
Table 10. Angle Step Test of LQR and MPC controllers, Controller input performance ( $U=19.45\text{ m/s}$ , $\theta = 22^\circ$ ).....	43
Table 11. Angle Step Test of LQR and MPC controllers, Error and model output performance ( $U=19.45\text{ m/s}$ , $\theta = 22^\circ$ ).....	43
Table 12. Lateral Distance Step Test of LQR and MPC controllers, Controller input performance ( $U=19.45\text{ m/s}$ , $R = 10$ , $\theta = 18.19^\circ$ ).....	44
Table 13. Lateral Distance Step Test of LQR and MPC controllers, Error and model output performance ( $U=19.45\text{ m/s}$ , $R = 10$ , $\theta = 18.19^\circ$ ).....	44

## NOMENCLATURE

### Symbols

$\psi, \dot{\psi}$	yaw angle and yaw rate of the vehicle
$v_x, v_y$	longitudinal velocity and lateral velocity in the body-fixed frame
$C_f, C_r$	cornering stiffness of the front and rear tires
$a_y$	lateral acceleration
$\rho$	radius of curvature
$t_r$	rise time
$t_p$	peak time
$t_s$	settling time
$e_{ss}$	steady-state error
$m$	Vehicle Weight
$I_z$	Vehicle Moment of Inertia (Z-Axis)
$a$	Distance between vehicle center of gravity and front axle
$b$	Distance between vehicle center of gravity and rear axle
$h$	The height of the vehicle's center of gravity from the ground
$U$	Longitudinal Velocity
$d$	half of vehicle tracks width
$C_{\alpha 1} = C_{\alpha 2}$	Front cornering stiffness
$C_{\alpha 3} = C_{\alpha 4}$	Rear cornering stiffness
$r_w$	Effective wheel radius
$g$	Gravity Constant

## **Abbreviations**

ADAS	Advanced Driver Assistance System
ULD	Unintended Lane Departure
S	Steering
B	Braking
S+B	Coordinated Steering and Braking
LKA	Lane-Keeping Assistance
LDW	Lane Departure Warning
LQR	Linear Quadratic Regulator
MPC	Model Predictive Controller
ARE	Algebraic Riccati Equation

# 1. INTRODUCTION

## 1.1. Literature Survey

The purpose of this chapter is to review the literature on the lane-departure prevention system. This introductory section briefly overviews vehicle safety and literature on Advanced Driver Assistance Systems (ADAS) functions, especially lane assistance systems. It then provides a brief market research and definition of the Unintended Lane Departure (ULD) problem. The last two sections briefly review the intervention methods and configurations and evaluate the intervention configurations' performance. The final section presents recent research on lane-keeping assistance control methods.

## 1.2. Safety Overview

In the automobile industry, safety is an important issue. National Highway Traffic and Safety Administration (NHTSA) reports that 42915 people died in 2021. The reported death rate for 2021 was the highest since 2007. Fatalities increased at a 10.5 percent rate compared to the year 2020. On average, each day, 117 people (one person every 7 minutes) died in 2021 [1]. The NHTSA says nearly 90 percent of crashes are associated with drivers' misunderstanding or inattention to the road environment [2]. According to the Turkish Statistical Institute [3] report, most traffic accidents are caused by driver mistakes. In order to reduce the number of crashes, Driver assist systems are being developed that can work in coordination with the driver and reduce the driver's workload without reducing driving stability and motivation [3].

Generally, motor vehicle crashes can be categorized into two classes. The first class relates to vehicle instability and is independent of the driver's commands. Examples are rolling over or spinning out. The second relates to the driver's commands and the environment—for example, unintended lane departure, lane crossing, head-on collisions, and crashes with road elements.

Similarly, vehicle safety systems available in the market can be categorized into two classes. First category overlooks vehicle stability by utilizing vehicle states merely. Examples include the anti-lock brake system (ABS) and electronic stability program (ESP). The other group assists the driver and focuses on environmental factors. Lane-keeping Assistance System (LKAS), Forward Collision Avoidance System (FCAS), Adaptive Cruise Control (ACC), and Parking Assistance System (PAS) are some

examples [4, 5]. Advanced Driver Assistance Systems inform the driver with alerts and/or intervene actively or utilize a combination of both to help the driver move away from trouble in case of distractions or misbehavior. It works in coordination with the driver while aiming not to affect the driving motivation negatively by taking control of the car unnecessarily but still able to avoid an obstacle even at the last moment by operating the vehicle within its actuator's physical limits.

This study has focused on Lane assistance systems. On average, about 4 to 10 percent of all crashes are related to lane changes [6]. To reduce crashes because of lane departure and upcoming hazards, before initiating a lane change must be aware drivers. Cicchino's studies show that LDW technology decreases the number of single-vehicle, sideswipe, and head-on collisions by eleven percent and accordingly decreases the number of injuries within this scope of crashes by 21 percent. One can indicate that if all cars were equipped with Lane Assistance technology, more than 55,000 injuries and approximately 85,000 official-reported collisions would have been prevented in 2015 [7].

### **1.3. Market Research**

The market can be segmented into Lane Departure Warning (LDW) and Lane Departure Prevention (LDP) systems. The LDW was the first lane departure assistance system developed for commercial trucks in 2000. The Lane Keeping Assistance (LKA) followed two years later [8] and is now available on most vehicles. LDW system provides visual, audible, and haptic alerts. In contrast, LDP or Lane Keeping Assistance (LKA) system automatically keeps the vehicle in its lane if the driver does not intervene after warnings. LKAS is an important candidate in the prevention of Lane Change crashes. Emergency Lane Keeping (ELK) system intervention is much more aggressive and intervenes when a critical situation is detected.

Nissan Cima was the first to offer an LDP assistance system (2001). Nissan's LDP alerts audible warning, followed by braking intervention on side wheels [9]. The selective application of the brakes helps keep the vehicle in the appropriate lane [10]. In another research, Nissan [11] also developed a Lane Keeping Control (LKC) system, which steers the vehicle back to its lane by applying steering torque in the case of lane departure.

Opel Eye (2010) and Ford Lane Keeping Alert (2012) systems developed a warning mechanism. When the unintended lane departure happens, the system alerts and makes

the driver aware of acting and returning the vehicle into its lane. Skoda Lane Assistant (2013), Audi Active Lane Assist (2012), Seat Lane Assist (2012), and Volkswagen Lane Assist (2010) systems, despite alerts, automatically initiate corrective steering, and the vehicle stays in the lane.

As mentioned, Some manufacturers prefer haptic or acoustic alerts while others intervene to recenter the vehicle into the lane. When lane crossing starts, intervention begins with automatically applied steering on front axle wheels or braking torque to the opposite wheels of travel direction. Market research surveys show that most LDP systems have recently applied steering angle control actuators to aid the vehicle back to its lane. This system rotates the steering column with an electric motor and steers the wheels.

Original equipment manufacturers (OEM) and aftermarket productions utilize the camera, laser, and infrared sensors, to detect lanes that apply to a wide range of vehicles, such as heavy commercial vehicles and passenger cars.

Finally, the ADAS market offers high growth opportunities, and leading manufacturers are investing in research and development to increase the safety of ADAS-equipped vehicles.

#### **1.4. Lane Departure Warning System**

Within years there have been lots of research on the Lane Departure Warning System (LDW) system to reduce the number of vehicle collisions. The LDW system warns the driver with visual, audible, and/or haptic feedback when the vehicle deviates from its lane [8, 12].

#### **1.5. Lane Keeping Assistance System**

The Lane Keeping Assistance (LKA) system is the driver assisting system that keeps the vehicle in the correct lane. These assistance systems aim to increase driving safety by preventing crashes [13].

Being different from the LDW system, lane keeping assistance (LKA) system is an active system attempting to keep the vehicle within the path of travel and orientated at the lane borders, while the lane centering system (LCA) orientating at the lane center and centering the vehicle in the lane [14]. LKA system is similar to line-tracking autonomous vehicles and employs the same scientific theories. There is a sensor which is generally a

video camera integrated in front of the vehicle, to recognize the lane markers. The vehicle's path is compared with the detected lane marker and steered automatically to keep the lane. However, a significant difference between LKA and Line Tracking Autonomous vehicles is a challenge: LKA requires both the system controller and the human driver to steer the vehicle together [15], which brings the necessity of using more complex algorithms.

The most common case which requires LKA to take control is when the vehicle departs from its lane without any intervention by the driver. This problem is named unintended lane departure (ULD).

### **1.6 Unintended Lane Departure Problem**

The Unintended Lane Departure (ULD) problem consists of two main parts: Detection and Reaction. In the detection phase, a supervisory controller evaluates the vehicle position relative to the road and determines whether there is a lane departure. The reaction phase starts when a departure is detected. In this phase, the driver alerts with a warning, and/or the controller intervenes in the vehicle state [16]. This study assumes that the controller will intervene to keep the vehicle in its lane.

A schematic of the ULD problem is given in Figure 1. It is assumed that the vehicle moves at a constant speed  $U$  and passes from a straight segment to a constant curvature segment of the road. Initially, the vehicle traveling direction is parallel to the road lane markers direction. The ULD controller commands the intervention, and there is no reaction from the driver. The controller starts to intervene on the vehicle states when lateral displacement between the vehicle center of gravity and the lane marker (lateral displacement error) exceeds the defined limit (50 centimeters). The objective of the intervention is to reduce the lateral displacement error to zero and center the vehicle on its lane. The lateral displacement error measurement is key to ensuring the successful implementation of ULD intervention and cannot exceed the shoulder width (3 meters).

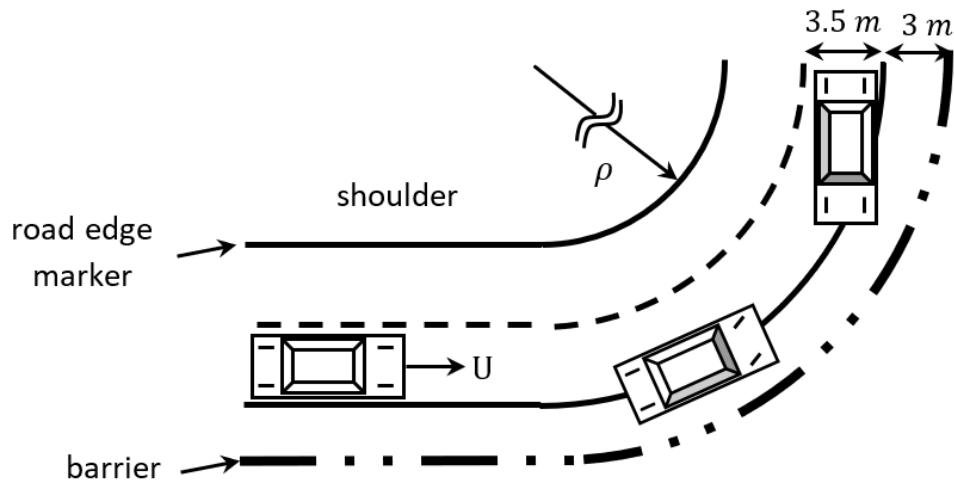


Figure 1. ULD problem schematic

### 1.7. Intervention Configurations

In the case of Unintended Lane Departure (ULD) or, more generally, Unintended Road Departure (URD), various intervention methods are used to ensure vehicle safety. The most common interventions are the use of Steering [17], Braking [10, 18], or traction torque [19]. Steering and braking systems can control one or more wheels. Both front steer and Four-Wheel Steer (4WS) methods let the driver control front axle wheels. However, 4WS has provided additional controls on the rear axle wheels, which are out of the driver's control. The brake system can independently apply corrective yaw moment to all wheels, thus steering the vehicle to its trajectory during maneuvers.

In a recent article, the front axle steering intervention method was experimentally tested on a prototype passenger car by Mammari et al. [17]. The study has covered the URD problem. Two main features are provided within this article. The first is tracking the road centerline, and the other is providing drive comfort by limiting the control inputs. A bicycle model was utilized for controller design. The controller outputs the required steering torque to the DC motor, which is mounted on the Electric Power Steering (EPS) column. When the controller activated, the driver could not apply any intervention input.

Another experimental study on the URD problem was conducted by Liu et al. [20] using the column-type EPS. The one-track bicycle model is used for controller design. Matlab/Simulink was used for performing the simulations on a straight road. It has been assumed that there is no intervention by the driver during the simulations. The



experimental tests were examined on the straight and curved test tracks with speed set to 100 km/h. According to the results, the designed intervention method has effectively been accomplished to keep the vehicle in its lane for a radius of curvature greater than 250 meters.

Kawazoe et al. [21] developed the lane-keeping system on a production prototype. The designed LKA system is intervened by front axle steering. This study has tested the effectiveness of LKAS on driver workload. The experiments were run with a test vehicle in which ACC was set at 100 Kph and driven on a specific route with the LKA system turned on and off for two hours. The results indicate that the driver workload was reduced to half when the system was on.

More recent attention has focused on the provision of rear axle steer intervention for lane keeping [22, 23]. Researchers selected the one-track vehicle model for designing the controller. Two additional states are added to the vehicle model to describe lane-keeping behavior. Rear axle steering is controlled with an extra control input. Rear axle steering is a function of vehicle velocity and front axle steering. This complex system can contribute to the vehicle's ability to cross severe maneuvers. Because of system complexity, the driver can steer the front axle, and rear axle steering is out of the driver's control. So, the ability to independently intervene on the vehicle steering is possible with the rear axle steering. Researchers developed control laws for both low and high-speed maneuvers. The results of this research indicate that rear axle steer intervention can reduce steady-state tracking errors.

There are few studies on the four-wheel steering (4WS) intervention method. Oya et al. [24] found that this method behaved robustly for simulations with variable vehicle velocity and removed the intervention oscillations. Paksincharoensak et al. [25] examined the performance of the lane-keeping system on straight and curved maneuvers with an active four-wheel-steering intervention method.

The study of preventing a vehicle from lane departing by applying yaw moment was carried out by Hayakawa et al. [26]. When lane departure happens, the system activates the brake on one side of the vehicle to correct this. This braking system can independently control the braking forces of the left and right wheels of the front and rear ends.

Nagai et al. [19] studied LKAS with the direct yaw moment control (DYC) intervention method. Researchers placed independently controlled small-size motors into each driving wheel to implement the DYC input. Lane-keeping theoretical behavior was studied using a linear 2-DOF vehicle model, while the observed behavior was examined with a micro-scale electric vehicle. The experimental tests and simulations show that the obtained results are highly consistent on the flat track and satisfactorily consistent on the curvy track. The yaw moment magnitude depends on several factors, such as road friction, vehicle slip angle, and maximum actuation travel.

Historically, research investigating the factors associated with four-wheel torque (4WT) intervention has focused on electric vehicles. Torque input can accelerate or decelerate each wheel independently. Lee et al. [27] studied the four-wheel torque control intervention method and tested it on an electric vehicle. A more robust approach to the independently controlled four-wheel drive electric vehicle can be found in Liang's article [28] on improving steering performance. Vehicle lateral stability was enhanced by unbalanced torque control at vehicle wheels, which caused yaw moment generation. Lateral steering was synthesized using the same method that was detailed for lateral stability. Researchers will study the coordination between lateral stability and steering performance by improving control of braking and traction behaviors of a four-wheel drive system for increasing vehicle safety and driving comfort.

Four-wheel steering and four-wheel torque (braking or traction) intervention methods support the notion that both methods have the potential to provide a corrective yaw moment. On the other hand, a literature search revealed few studies on driver comfort [29, 30]. These studies show that brake actuation causes pedal vibration, deceleration, and modulator noise during yaw moment generation. However, the 4WS has unnoticeable haptic or audible feedback and incomprehensible deceleration. So, the 4WS system has a lower level of disturbance to the driver. These findings imply that each intervention method has its benefits and strengths, but it is worth losing some benefits in order to obtain many others. The combination of these methods in the coordinated intervention case provides the benefits of both methods. Therefore, the actuator workload decreased and was distributed between the brake and steering. The most prominent finding to emerge from the analysis is that the vehicle performs better deceleration, less side-slip angle, and improved stability. The first serious discussions and analyses of steering and

braking intervention methods comparison were studied by Alleyne in 1997. Alleyne has studied different types of intervention which are 1) Four Wheel Steering, 2) Front Wheel Steering, 3) Four Wheel Brake Steering, 4) Front Wheel Brake Steering. and 5) Rear Wheel Brake Steering [16].

While slightly different configurations exist, four wheels independent braking and front steering are used for a vehicle lateral dynamic control approach [31]. The research aims to obtain the nominal behavior of the vehicle while tracking the given reference as close as possible. In the case of ULD, it is intended to maintain the directional stability with the steering system. In contrast, the braking system could provide a yaw moment even if it is not as effective as slowing down the vehicle. It is aimed to improve the vehicle performance on ULD maneuvers by coordinating the brake and steering systems. Therefore, it aimed to eliminate conflicts between systems to take advantage of the strengths of each component.

On the technical side of the rear steering and 4WS systems, there is a lack of precise and, at the same time, inexpensive solutions for the LKA intervention. The 4WB is like Electronic Stability System (ESP), which can control each wheel braking independently. The front steering system is available with Electronic power steering (EPS) system on recent vehicles. As a result, front steering is almost as feasible to apply as 4WB. Coordinating these systems is another topic for study. There are few historical studies on coordinated 4WS (4 Wheel Steer) and braking intervention methods.

Within the scope of this thesis, directional intervention with front axle steering and rear axle braking is open to development. Hence this configuration is developed and validated under different test cases. Detailed information about the configuration and test cases are presented in the following chapters.

## **1.8. Control Methods**

This section investigates control methods that interfere with the ULD problem. Different theories exist in the literature regarding lane-keeping system control algorithms. The first serious discussions and analyses of automated steering for lane keeping emerged during the 1960s with Gardels [32] and Cardew [33]. Investigating automatic lane-keeping is a continuing concern for research in this area. Fenton et al. [34] designed the control algorithms using classical control methods and validated their designs through

experiments in the late 1970s. This paper has focused on the disturbance rejection capability of the feedback controller, likewise Alleyne's [35] study to track curved roads. From the late 1980s and culminating to date, the LKA has received much attention under vehicle automation on the highway.

A comparison of  $H_\infty$ , adaptive, fuzzy, and PID controllers was studied by Mammar et al. [36]. The linearized lateral vehicle model [37] was used to design controllers. The steering angle is selected as the intervention input. Simulations consist of changes in vehicle speed and road friction coefficient, corruptive factors such as wind and road curvature performed a comparison of controllers. The results show that the proportional controller is least affected by wind force while presenting the most significant error. The self-tuning regulator, despite wind force, presents the best response and the smallest error. The  $H_\infty$  and Fuzzy controllers have equivalent performances. Although the self-tuning regulator, which is the most complex controller, presents the best performance. Finally, the errors increase as the friction coefficient decreases and speed increases. In the same manner, researchers used a single-track model in the design of the controller and neglected the effect of road curvature [17]. Driver steering and assistant steering torques are used as system inputs in a coordinated manner. The Linear Matrix Inequalities (LMI) technique based on Lyapunov theory is used for controller design. The controller was examined on a prototype vehicle, and a control signal was applied when the ULD happened. Experiments show that the controller can take the vehicle in its lane in a typical driving situation.

Liang et al. [28] developed a detailed vehicle model for improving the performance of steering system control on 4WD electric vehicles. The controller achieved increasing high-speed stability and low-speed comfort with unbalanced torque control on each wheel for generating the required yaw moment. The yaw moment is calculated with  $H_\infty$  and optimized by Moore–Penrose theory.

The technique of obtaining a robust controller for lateral vehicle control was studied by Cerone and Regruto [37, 38]. The obtained model has a single input and two outputs (SITO). The steering angle is controlled with a motor. The model input is the control signal which controls the vehicle steering angle. The model outputs are the vehicle's lateral position and heading angle with respect to the lane center. For the simple design of the proposed SITO controller, researchers reduced the SITO control problem into a

SISO (Single Input- Single Output) and then designed the required controller. In order to design a robust controller,  $\mu$ -synthesis method applied. Experimental results on the highway, including straight and curved tests, are satisfactory.

The findings suggest that the LKA is a multivariable (MIMO) system. The notion of optimality is closely tied to the MIMO control system design. In this sense, the LQR provides an automated design procedure, a well-known design technique that provides practical feedback gains. Fenton et al. [39] explored the linear–quadratic (LQ) approach in the 1980s, which may be the first laboratory study to simulate vehicle dynamics using an analog computer. In the late 1990s, Alleyne’s (Alleyne, 1997) study of LQR performance on different intervention configurations was the most intriguing. This rather exciting finding could be due to examining LQR controller performance on different intervention configurations. Likewise, in Fenton's work, the controller was designed using a simplified two-degrees-of-freedom single-track vehicle model and examined with a non-linear vehicle model with seven degrees of freedom.

More recently, Freeman et al. [40] investigated SL (Sliding), LQ (Linear Quadratic), and control methods based on classical control theory for the dynamic control of the vehicle in case of road departure. An implication of this comparison used nonlinear two-track and linear one-track vehicle models for controller design. Intervention applied by steering and braking actuators. During the intervention, it is assumed that the traction torque generation on wheels was neglected and set to zero. Contrarily, steering and brake torque can be applied by a wired system. The steering angle intervention applies a significant part of the intervention required to bring the vehicle back to the road. At the same time, independent braking triggers proper intervention to achieve the desired yaw moment stability. Matlab’s Simulink and CarSim were selected as simulation software. The results show that LQ and SL controller methods have maintained vehicle stability better than other controllers.

Bian et al. set out to find a new method for the combination of vehicle lateral and longitudinal control for lane-keeping and speed tracking, respectively [41]. To examine the performance of the combined control method, researchers carried out a series of experiments on the four-wheel steering (4WS) and driving (4WD) electric vehicle. The nonlinear vehicle dynamics were obtained with the Takagi-Sugeno (T-S) fuzzy model. The steering angles and motors located inside the wheels for generating traction and brake

torque had limitations due to their design features. The MPC controller was selected to overcome these actuator limitations and ensure the control performance. The designed controller was examined with simulations prepared in CarSim and Simulink. The fuzzy MPC (FMPC) controller performs successfully on the curved road with variable speed.

Explicit Model Predictive Control (eMPC) for the lane-keeping system was studied by Lee and Chang [42]. This controller's principal objective was to control an autonomous vehicle's steering angle along desired paths. Tests were carried out on straight, circular, and clothoid paths. A comparison between eMPC, MPC, and LQR control methods is presented, and the performance of the proposed controller is proved. CarSim is selected as a vehicle model for simulations.

Similarly, Turri et al. [43] studied Linear MPC performance for the LKA approach on highways. Independently controlled braking and front steering actuators oriented the vehicle on its desired path. Researchers set up a series of virtual simulations and experimental tests to examine the controller's performance. The experimental Test results with a passenger car on a snowy road reveal that the designed controller performed successfully.

In the late 1960s, the receding horizon control received scant attention in the research literature. LQR and MPC have become common trends in vehicle dynamic control systems. There are similarities between the design procedures of LQR and MPC, and there is a crucial difference between their solution horizons. In comparison, the LQR has a single solution for the whole horizon, while MPC optimizes the solutions at each step of the prediction horizon. To date, large-scale studies have been performed to investigate the prevalence of MPC in optimal control. With successive increases in the application of the MPC, the LQR has received lower scant attention from scholars.

## **1.9. Conclusion**

This chapter presents a literature survey on Lane Departure Assistance Systems (LDAS) and analyses the applied controller structures. First, market research about available lane-departure assistance systems indicates automakers use steering and braking intervention methods. Parallely, a review of the most common intervention methods shows that the intervention can be applied via steering or braking actuators. As a result of investigations about different combinations of intervention methods, steering is the most preferred

method. Finally, the literature survey demonstrates a lack of coordinated intervention between the steering and braking approaches, which is the focus of this dissertation in chapter 2.

## **2. THEORETICAL BACKGROUND**

### **2.1. Intervention Configuration**

The literature survey on intervention configuration methods demonstrates a lack of coordinated intervention between the steering and braking. Therefore, this study focuses on developing a novel intervention configuration with higher applicability for the LKAS system. Furthermore, an Examination of preferred configurations in the market demonstrates that interventions were generally performed by braking the two (front and rear) wheels on the opposite side of the abandoned lane line or steering the vehicle's front axle. Therefore, at the moment of any intervention, at most, two wheels generate lateral force to control the vehicle in the lane.

In addition, research shows that the 4WS and 4WB methods are costly because of their complex actuator control requirements. Especially the 4WS method requires steering control of the rear axle, which applies to particular vehicle types. On the other hand, the 4WB method application is realistic because it can use available brake actuators. However, the performance is slightly similar to a one-axle braking method which uses two brake actuators instead of four [16]. Last but not least, the lack of coordinated intervention between the steering and braking approaches becomes more apparent. This configuration combines front-wheel steering with rear-axle braking (briefly S+B configuration) and, thanks to its capability to use three wheels' force potential, increases the overall intervention's robustness, making it applicable in all situations, such as understeer or oversteer. Thus, its application is possible without needing an extra actuator. Also, each wheel is under control using only one actuator, and the control of the actuators is not complicated. These features make the (S+B) approach more efficient. However, this novel approach requires a validation check to corroborate its performance. The Simulink and CarMaker software were selected for the virtual simulation of performance tests. Hence, the next sections focus on the vehicle model and controller design for the preparation of the virtual test.

### **2.2. Vehicle Model**

A single-track vehicle model was used in the controller design and designed controller tested on a nonlinear simulation model using the CarMaker software of IPG company. This software consists of road, driver, and vehicle models and can virtually reflect real-



life behaviors. Another feature is that it can work together with equations of motion, kinematics, and other vehicle dynamics. In addition, since it can work in coordination with the Matlab-Simulink program, the desired simple and complex maneuvers are realized. In this study, since the driver is assumed not to intervene, the driver model is disabled, and the designed controller provides the vehicle control input.

The vehicle model consists of tires, brakes, steering, and other components. Tires contribute significantly to the vehicle's dynamics by generating forces and moments in the tire-road contact, which can alter the speed and orientation of the vehicle. Therefore, several mathematical tire models were developed to quantify the forces and moments and examine the vehicle's dynamic behavior. The CarMaker used a nonlinear tire model based on Pacejka's [44] Magic Formula equations.

Due to the nature of the intervention configuration, only the dynamics of the rear axle brake module are modeled (see Figure 2).

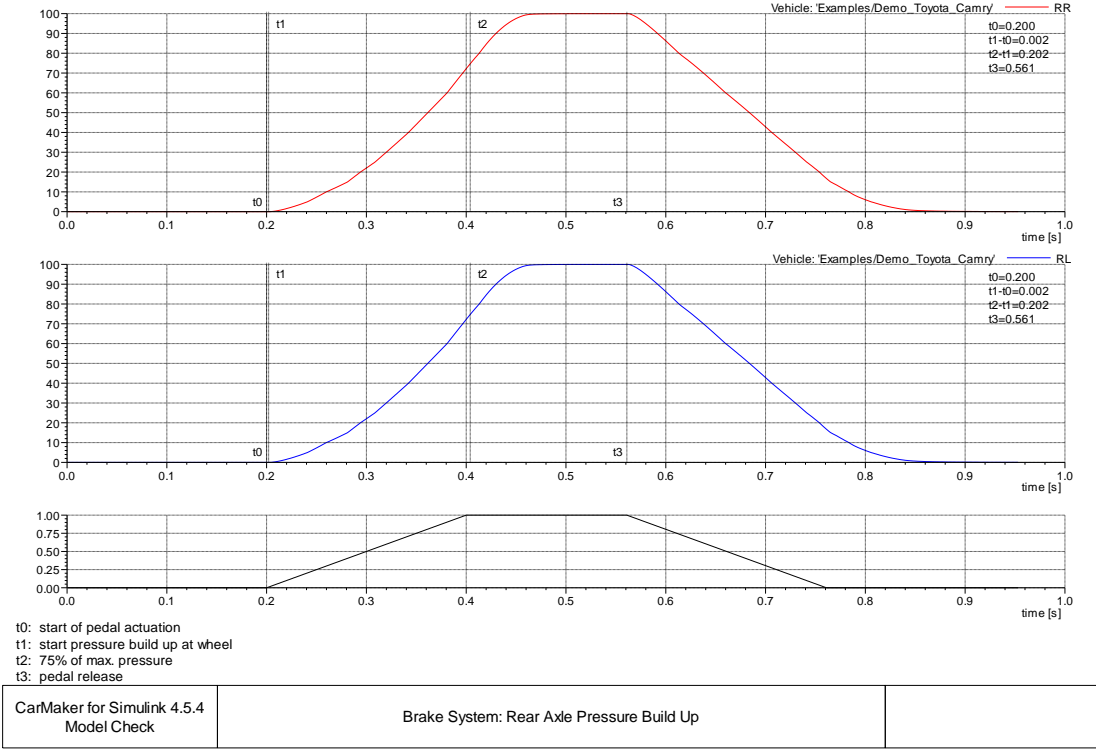


Figure 2. Rear-axle brake pressure build-up of CarMaker model (Response time = 0.005[s] , Build-up time = 0.08[s])

Performing step response tests revealed at least a second order and critical or over-damped relationship between pedal input and the resulting braking torque. The time constant determined in the brake step response tests is 0.0577s. Therefore, brake hydraulic system dynamics are modeled as a first-order filter using this time constant.

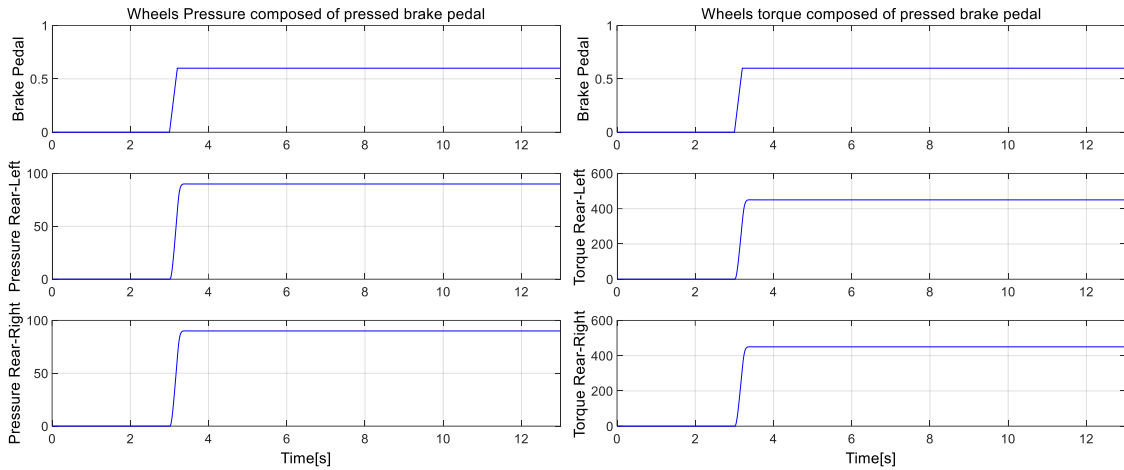


Figure 3. Step response test of the brake pedal

By using the sinus sweep test (see Figure 4), it was determined that the steering angle bandwidth was in the order of 2 Hz. However, the steering model's response frequency was considered one Hz in the simulation tests. Therefore, the steering system dynamic is modeled as a first-order filter with a time constant of 0.1 s.

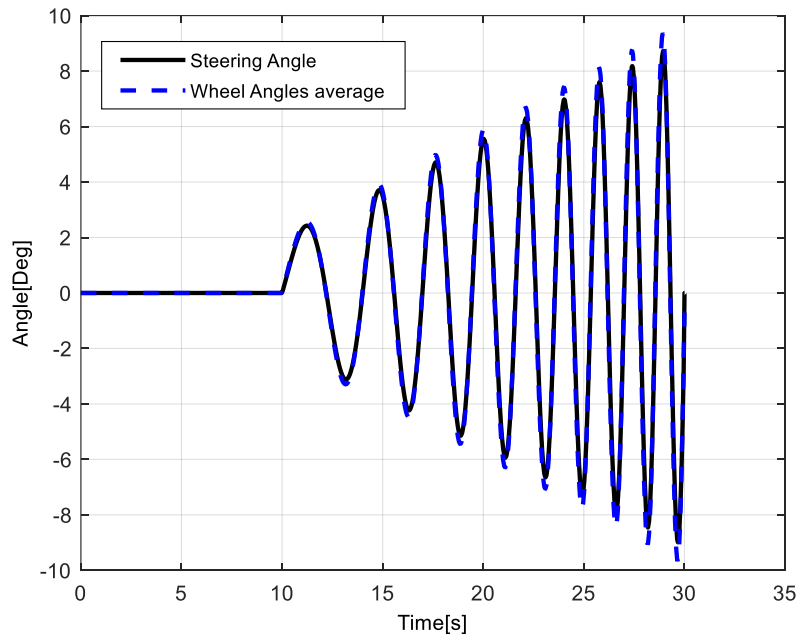


Figure 4. Sine sweep test of the steering system

### 2.3. Road Model

In this study, the width of each lane is defined as 3.5 meters, and the width of the road shoulders is 2.5 meters under the Highway Geometric Standards Principles [45]. In addition, in the tests carried out at 100 and 80 km/h, the minimum radius of the road curvature was defined as 400 and 250 meters, respectively.

### 2.4. Controller Design

The Lane Keeping Assistance System (LKAS) of a vehicle attempts to keep the vehicle between lanes despite disturbances caused by changing the curvature of the road and variations in the road conditions. The system measures the trajectory tracking error and adjusts steering or braking to generate a yaw moment.

In this thesis, the linear quadratic regulator (LQR) and model predictive control (MPC) were implemented on Matlab to control the vehicle model in CarMaker software. These controllers' primary objective is to minimize the vehicle trajectory deviation between lanes. This part provides a brief derivation of the LQR and MPC controllers.

#### 2.4.1. Linearized vehicle model

Vehicle modeling has an important place in the analysis of dynamics, and the more precise the model, the closer the simulation results will be to reality. This section presents two dynamic models for controller design: the one-track and the two-track models. The schematic given in Figure 5 is a two-track vehicle model diagram.

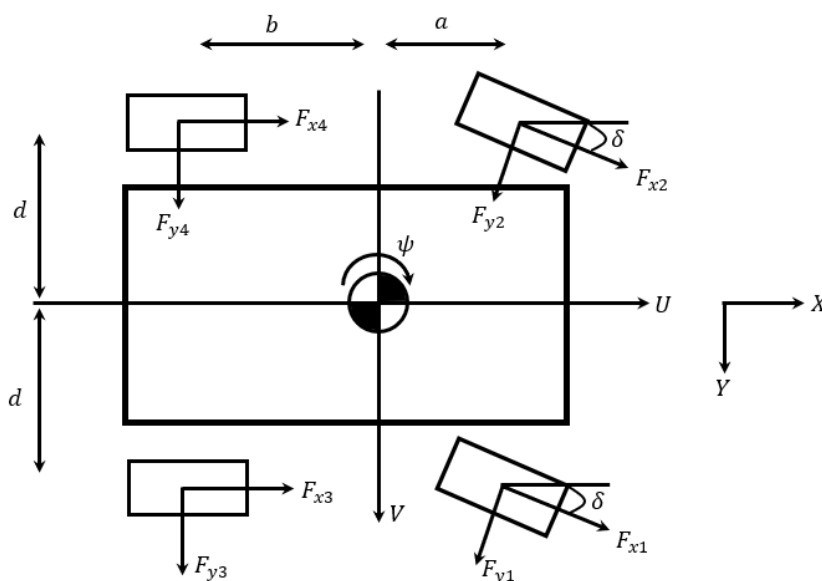


Figure 5. Simple two-track Lateral Vehicle Model

The single-track vehicle model, also known as the bicycle model, is the simplest dynamic vehicle model, replacing two wheels per axle with one single wheel. Figure 6 presents the single-track model in which the longitudinal speed of the vehicle is considered constant and this assumption decreases the degree of freedom to 2, thus simplifying the problem.

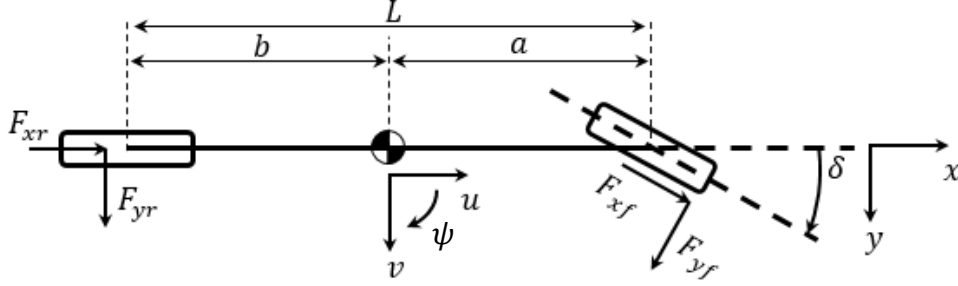


Figure 6. One-track Vehicle Model

The equations of motions for Longitudinal (1), Lateral (2), and yaw (3) are presented:

$$\dot{U} = 0, U = U(t = 0) = \text{constant} \quad (1)$$

$$\sum F_y: m(\dot{V} + \psi U) = F_{y1} + F_{y2} + F_{y3} + F_{y4} \quad (2)$$

$$\sum I_z \dot{\psi} = a(F_{y1} + F_{y2}) - b(F_{y3} + F_{y4}) + d(F_{x2} + F_{x4}) - d(F_{x1} + F_{x3}) \quad (3)$$

In this model, the lateral wheel forces are proportional to the wheel slip angle,

$$F_{yi} = C_{\alpha i} \alpha_i \quad i \in \{1, 4\} \quad (4)$$

$C_{\alpha i}$  is the cornering stiffness parameter. Combine the tire cornering stiffness values for the single-track inequalities for each wheel.

$$C_{\alpha f} = C_{\alpha 1} + C_{\alpha 2} \quad (5)$$

$$C_{\alpha r} = C_{\alpha 3} + C_{\alpha 4}$$

The longitudinal forces are directly proportional to the braking torque force inputs applied to the vehicle.

$$F_{xi} = \frac{T_{bi}}{r_{\omega i}} \quad i \in \{1, 4\} \quad (6)$$

$$x_i = F_{xi} - F_{yi} \delta_i \quad i \in \{1, 4\}$$

$$y_i = F_{xi} \delta_i + F_{yi} \quad i \in \{1, 4\}$$

The simplified version of wheel slip angles:

$$\alpha_1 = \frac{v + a\psi}{U} - \delta; \alpha_2 = \frac{v + a\psi}{U} - \delta; \alpha_3 = \frac{v - b\psi}{U}; \alpha_4 = \frac{v - b\psi}{U}; \quad (7)$$

The vehicle dynamics created by using all these inequalities together are re-written as:

$$m(\dot{V} + \psi U) = \frac{C_{\alpha f} + C_{\alpha r}}{U} V + \frac{aC_{\alpha f} - bC_{\alpha r}}{U} r + (F_{x1} + F_{x2} - C_{\alpha r})\delta \quad (8)$$

$$I_z \dot{\psi} = \frac{aC_{\alpha f} - bC_{\alpha r}}{U} V + \frac{a^2 C_{\alpha f} + b^2 C_{\alpha r}}{U} r + a(F_{x1} + F_{x2} - C_{\alpha f})\delta - d(F_{x3} - F_{x4}) \quad (9)$$

The last term of the equation written for yaw motion is negligible because it is very small compared to the other terms. Then, torque inputs are substituted for longitudinal forces in the inequality, and the final deviation inequality takes the form:

$$I_z \dot{\psi} = \frac{aC_{\alpha f} - bC_{\alpha r}}{U} V + \frac{a^2 C_{\alpha f} + b^2 C_{\alpha r}}{U} \psi - aC_{\alpha f} \delta - d \left( \frac{T_{b3}}{r_{w3}} - \frac{T_{b4}}{r_{w4}} \right) \quad (10)$$

A model that considers the car's position and orientation error relative to the road is required to create a steering control system for automatic lane-keeping. Peng ve Tomizuka [46] redefined the system states and motion inequalities to develop a model for lane tracking:

$$\frac{d}{dt} \begin{bmatrix} e \\ \dot{e} \\ \Delta\psi \\ \Delta\dot{\psi} \end{bmatrix} = \begin{bmatrix} 0 & 1 & 0 & 0 \\ 0 & \frac{C_{\alpha f} + C_{\alpha r}}{mU} & -\frac{C_{\alpha f} + C_{\alpha r}}{m} & \frac{aC_{\alpha f} - bC_{\alpha r}}{mU} \\ 0 & 0 & 0 & 1 \\ 0 & \frac{aC_{\alpha f} - bC_{\alpha r}}{I_z U} & -\frac{aC_{\alpha f} - bC_{\alpha r}}{I_z} & \frac{a^2 C_{\alpha f} + b^2 C_{\alpha r}}{I_z U} \end{bmatrix} \begin{bmatrix} e \\ \dot{e} \\ \Delta\psi \\ \Delta\dot{\psi} \end{bmatrix} \quad (11)$$

$$+ \begin{bmatrix} 0 & 0 \\ -\frac{C_{\alpha f}}{m} & 0 \\ 0 & 0 \\ -\frac{aC_{\alpha f}}{I_z} & -\frac{d}{r_{\omega} I_z} \end{bmatrix} \begin{bmatrix} \delta_f \\ T_{Bs} \end{bmatrix} + \begin{bmatrix} 0 & 0 \\ \frac{aC_{\alpha f} - bC_{\alpha r}}{m} - U^2 & 0 \\ 0 & 0 \\ \frac{a^2 C_{\alpha f} + b^2 C_{\alpha r}}{I_z} & 0 \end{bmatrix} \frac{1}{\rho}$$

In the inequality, the vertical distance from the road edge ( $e$ ), the angular difference between the straight road segment, and the projection of the vehicle's longitudinal axis ( $\Delta\psi$ ).

The road curvature is a disturbance to the system, and its tracking is considered to regulate a lateral displacement and track a yaw rate. If the radius of curvature of the road is constant, the yaw rate difference between the vehicle and the road can be easily calculated:

$$\Delta\dot{\psi} = r_{vehicle} - r_{road} = r_{vehicle} - \int_0^t \frac{U(\tau)}{\rho} d\tau \quad (12)$$

The disturbance term is a constant with a constant longitudinal velocity assumption. Therefore, the standard Linear Quadratic method [47] to regulate the system about the state space origin involves minimizing the cost function.

$$J = x^T(t_f)Sx(t_f) + \int_{t_0}^{t_f} (x^T(\tau)Qx(\tau) + u^T(\tau)Ru(\tau))d\tau, X \in \mathfrak{R}^n, u \in \mathfrak{R}^m \quad (13)$$

Ricotti inequality solved for linear, time-independent feedback.

$$A^T H + HA - HBR^{-1}B^T H + Q = 0 \quad (14)$$

With the arranged inequalities, the following equations can be written:

$$U = -(R^{-1}B^T H)x = -K_{FB}x, K_{FB} \in \mathfrak{R}^{1 \times n} \quad (15)$$

$$u_{tracking} = -K_{FB}x + K_I \int_0^t x d\tau, K_{FB}, K_I \in \mathfrak{R}^{1 \times n}$$

In this study, the system dynamics were redefined by adding the integral of the lateral error as a state and explicitly included in the LQ weighting matrices. As a result, the corresponding equation is given:

$$\frac{d}{dt} \begin{bmatrix} \int e \\ e \\ \dot{e} \\ \Delta\psi \\ \Delta\dot{\psi} \end{bmatrix} = \begin{bmatrix} 0 & 1 & 0 & 0 & 0 \\ 0 & 0 & 1 & 0 & 0 \\ 0 & 0 & \frac{C_{af} + C_{ar}}{mU} & -\frac{C_{af} + C_{ar}}{m} & \frac{aC_{af} - bC_{ar}}{mU} \\ 0 & 0 & 0 & 0 & 1 \\ 0 & 0 & \frac{aC_{af} - bC_{ar}}{I_z U} & -\frac{aC_{af} - bC_{ar}}{I_z} & \frac{a^2 C_{af} + b^2 C_{ar}}{I_z U} \end{bmatrix} \begin{bmatrix} \int e \\ e \\ \dot{e} \\ \Delta\psi \\ \Delta\dot{\psi} \end{bmatrix} + \begin{bmatrix} 0 & 0 \\ -\frac{C_{af}}{m} & 0 \\ 0 & 0 \\ -\frac{aC_{af}}{I_z} & -\frac{d}{r_{\omega} I_z} \end{bmatrix} \begin{bmatrix} \delta_f \\ T_{Bs} \end{bmatrix} + \begin{bmatrix} 0 \\ 0 \\ \frac{aC_{af} - bC_{ar}}{m} - U^2 \\ 0 \\ \frac{a^2 C_{af} + b^2 C_{ar}}{I_z} \end{bmatrix} \frac{1}{\rho} \quad (16)$$

If we design a state feedback controller, then we can regulate the system using the feedback input:

$$u = -Kx$$

It is easy to see that the error dynamics are identical to the system dynamics, and in this case, we do not need to schedule the gain based on states( $x$ ); one can compute a constant feedback gain  $K$ .

#### 2.4.2. Linear Quadratic Regulator

Optimal control, as one of the modern methods of control, has a special place in the discussion of control systems. One of the optimal control methods is the Linear Quadratic Regulator [48], abbreviated as LQR. This method is optimized for linear systems and successfully ensures system stability in many applications due to the straightforward design process and simple structure. Although the LQR method can also be applied to nonlinear systems using Jacobi linearization, the controller is no longer optimal but performs well in most applications.

The optimal control problem works with the minimization of a cost function. This functional equation measures the performance of a control model that quantifies the cost of making that controller to minimize input energy and maximize output efficiency.

In this section, the infinite horizon linear quadratic regulator (LQR) problem is defined for a system described in state-space form by:

$$\dot{x}(t) = Ax(t) + Bu(t)$$

Where  $A, B$  matrices are the model matrices obtained by the System Identification. Find the control input  $u(t), t \in [0; \infty)$  that makes the following cost function as small as possible:

$$J_{LQR} = \int_0^{\infty} (x^T Q x + u^T R u) dt$$

where  $Q \geq 0$  and  $R > 0$  are symmetric, positive-semi-definite and positive-definite matrices respectively. Term  $x^T Q x$  corresponds to the state cost and  $u^T R u$  corresponds to the control cost. LQR seeks a controller that minimizes both terms.

The diagonal  $Q$  and  $R$  matrices are selected simply and reasonably with Bryson's rule [49]:

$$q_{ii} = \frac{1}{\text{maximum acceptable value of } x_i^2}$$

$$r_{jj} = \frac{1}{\text{maximum acceptable value of } u_j^2}$$

So, the  $Q$  and  $R$  matrices are:

$$Q_{l \times l} = \begin{bmatrix} q_{11} & 0 & 0 \\ 0 & \ddots & 0 \\ 0 & 0 & q_{ii} \end{bmatrix} \quad R_{m \times m} = \rho \begin{bmatrix} r_{11} & 0 & 0 \\ 0 & \ddots & 0 \\ 0 & 0 & r_{jj} \end{bmatrix}$$

For optimization of the cost function, the following partial differential equation, which is known as the Hamilton Jacobi Bellman Equation (Hamiltonian equation) used:

$$H = x^T Q x + u^T R u + \lambda^T (Ax + Bu)$$

Where  $\lambda$  is the Lagrange multiplier, the necessary conditions for optimality are:

$$\text{Co-State equation: } \dot{x} = \left(\frac{\partial H}{\partial \lambda}\right) = Ax + Bu \quad x(0) = x_o$$

$$\text{Co-state Equation: } \dot{\lambda} = -\left(\frac{\partial H}{\partial x}\right) = -(Qx + A^T \lambda) \quad \lambda = Px$$

$$\text{Optimal control equation: } \frac{\partial H}{\partial u} = 0 = Ru + \lambda^T B \implies u = -R^{-1} B^T \lambda$$

Guess the form of the solution,  $\lambda = Px$ . From the functional analysis theory of normed linear space [50],  $\lambda(t)$  lies in the "dual space" of  $x(t)$ , which is the space consisting of all continuous linear functionals of  $x(t)$ . This gives the optimal solution. Then:

$$\begin{aligned} \dot{\lambda} &= \dot{P}x + P\dot{x} = \dot{P}x + P(Ax + Bu) = \dot{P}x + P(Ax - BR^{-1}B^T P)x \\ &(\dot{P} + PA - PBR^{-1}B^T P)x = -(Qx + A^T Px) \end{aligned}$$

This equation is satisfied if we solve Differential Riccati Equation and find  $P$  such that

$$(\dot{P} + PA + A^T P - PBR^{-1}B^T P + Q)x = 0$$

where in the infinite horizon  $P$  is the solution of the Algebraic Riccati Equation (ARE):

$$PA + A^T P - PBR^{-1}B^T P + Q = 0$$

Furthermore, the optimal control input computed:

$$u = -R^{-1} B^T P x$$

In this thesis, the LQR controller minimizes the cost of states and controller inputs to keep the vehicle in its desired lane. Bryson's rule is used for obtaining the  $Q$  and  $R$  matrices. The components used in  $u$  and  $x$  have different units, so with scaling the variables of  $J_{LQR}$  with Bryson's rule, the maximum acceptable value for each term becomes one. Although Bryson's rule usually gives good results as an initial guess for the heuristic approach of designing the optimal controller. Choose each  $q_i$  such that ( $e$  distance in meters,  $\psi$  angle in radians):



$$\begin{aligned}
\int e \rightarrow 3ms \text{ error OK} &\Rightarrow q_{11} = \left(\frac{1}{3}\right)^2 \approx 0.1 & q_1 x_1^2 = 1 \text{ when } x_1 = 3 \text{ ms} \\
e \rightarrow 1m \text{ error OK} &\Rightarrow q_{22} = \left(\frac{1}{1}\right)^2 = 1 & q_2 x_2^2 = 1 \text{ when } x_2 = 1 \text{ m} \\
\dot{e} \rightarrow 1 \frac{m}{s} \text{ error OK} &\Rightarrow q_{33} = \left(\frac{1}{1}\right)^2 = 1 & q_3 x_3^2 = 1 \text{ when } x_3 = 1 \frac{m}{s} \\
\Delta\psi \rightarrow 0.1rad \text{ difference OK} &\Rightarrow q_{44} = \left(\frac{1}{0.1}\right)^2 = 100 & q_4 x_4^2 = 1 \text{ when } x_4 = \frac{1}{10} \text{ rad} \\
\Delta\dot{\psi} \rightarrow 0.1 \frac{rad}{s} \text{ difference OK} &\Rightarrow q_{55} = \left(\frac{1}{0.1}\right)^2 = 100 & q_5 x_5^2 = 1 \text{ when } x_5 = \frac{1}{10} \frac{rad}{s}
\end{aligned}$$

Similarly, with  $r_i$ :

$$\begin{aligned}
\delta_f \rightarrow 40^\circ \text{ Steering} &\Rightarrow r_1 = \left(\frac{1}{40 \times \frac{\pi}{180}}\right)^2 \approx 2 & r_1 u_1^2 = 1 \text{ when } u_1 = 40^\circ \\
T_{Bs} \rightarrow 1000 \text{ Nm Braking Torque} &\Rightarrow r_2 = \left(\frac{1}{1000}\right)^2 = 10^{-6} & r_2 u_2^2 = 1 \text{ when } u_2 = 1000 \text{ Nm}
\end{aligned}$$

Use  $\rho$  to adjust input/state balance

$$\rho = 1$$

The next attempt is to regulate the weights of  $Q$  and  $R$  and find  $P$  such that the Riccati equation converge. In this study  $Q$  and  $R$  matrices were selected as below:

$$Q = \begin{bmatrix} 0.1 & 0 & 0 & 0 & 0 \\ 0 & 1 & 0 & 0 & 0 \\ 0 & 0 & 1 & 0 & 0 \\ 0 & 0 & 0 & 100 & 0 \\ 0 & 0 & 0 & 0 & 100 \end{bmatrix}; \quad R = \begin{bmatrix} 2 & 0 \\ 0 & 10^{-6} \end{bmatrix}$$

By selecting cheaper control costs, the energy and effort of the system increase. In addition, applying sudden hard braking may cause instability. Therefore, the maximum acceptable value of braking changed to 100Nm with the trail-and-error method:

$$R = \begin{bmatrix} 2 & 0 \\ 0 & 10^{-4} \end{bmatrix}$$

Solve the ARE for the selected  $Q$  and  $R$  matrices:

$$PA + A^T P - PBR^{-1}B^T P + Q = 0$$

Then calculate the gain matrix of the feedback controller by:

$$K_{FB} = -R^{-1}B^T P$$

### 2.4.3. Model Predictive Control

Model Predictive Control (MPC) is a trending strategy for the control of multi-input multi-output systems. MPC is closely related to the LQR controller described in Section 2.2.1. Recently, the popularity of MPC for industrial and academic applications has increased. The reason is that MPC designs can produce high-performance control systems that can operate with intervention over a future time horizon. The MPC allows stating constraints and predicting control output signals and states, which can give the controller insight into several attributes of the controlled system, e.g., physical restrictions on the input signal. MPC is a control technique with the fundamental idea of using a model of the system to predict its behavior up to a specific prediction horizon and generating control inputs that satisfy the constraints and minimize a cost function

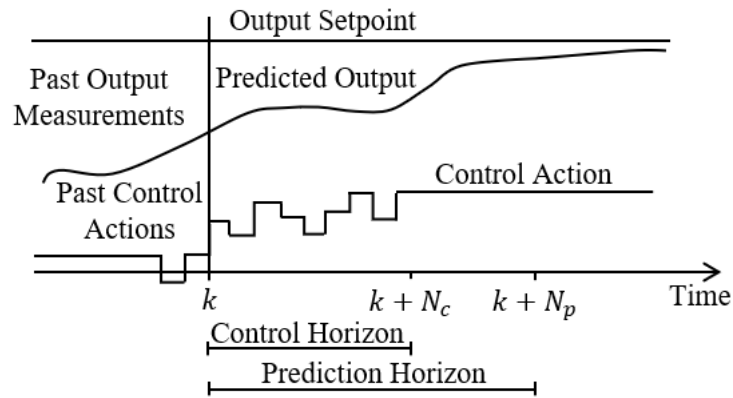


Figure 7. General MPC scheme at  $k$ 'th step

Figure 7 shows the general MPC scheme at time  $k$ .  $N_p$  and  $N_c$  symbols imply the control horizon and prediction horizon, respectively. To clarify the terms, prediction horizon ( $N_p$ ) can be described as number of future samples for the prediction of plant output and control horizon ( $N_c$ ) is the number of samples within the prediction horizon to capture the control action. As a note,  $N_c$  can be less than or equal to  $N_p$ . Since the lengths of these parameters directly affect the complexity of the problem and system performance, some samples should be selected to provide the optimal solution. The vehicle can look ahead for fifty seconds, which is the product of the prediction horizon and sample time. This look-ahead time enables the controller to use previewed information to calculate controller inputs, improving the MPC controller performance. The control horizon is two meters.

Four headings summarize the critical elements of the MPC algorithm:

- Plant Model

- Prediction of Outputs
- Cost function
- Constraints

Detailed information about the MPC design steps and headings is in Appendix 2. In this thesis, it is planned to program the MPC with the introduced code in Appendix 2. “MPCQPSOLVER” was introduced in the Matlab R2015b version; however, the available CarMaker version works with the Matlab R2014b, so it was impossible to use the code. Instead, using the MPC toolbox in the R2014b Simulink, a controller was designed, and its performance was checked with available code in Matlab R2022b. They perform very similarly.

## **2.5. Conclusion**

This chapter demonstrates that a novel coordinated steering and braking approach increases the performance of the LKA system by using the force potential of three wheels compared to only braking and only steering interventions using the force potential of two wheels. Using simulation tools is one of the best low-cost methods for performing comparison tests. The Simulink and CarMaker Software provide a virtual simulation environment to repeat the same test scenarios several times. The following chapters demonstrate the step response [49] test scenarios in which the KPIs (key performance indicators) are defined. For performing tests, the MPC and LQR controllers are prepared to control the virtual vehicle model and provide the required control input in the CarMaker simulation environment.

### 3. SIMULATION EXPERIMENT DESIGN

Recently, one of the safe methods for examining driver assistance functions performance is the simulation. Simulation tools like The CarMaker software could simulate a vehicle's dynamic behavior, including all its components like ADAS sensors, steering system, brakes, and tires. Furthermore, the tool includes road and environmental modeling capability. With this capability, it is possible to implement step and ramp response test scenarios in the simulation. The most commonly used method to measure a dynamic system's performance is to examine the system's step and ramp response due to its ease of use and analysis. Therefore, these test scenarios examine the controller's and intervention configuration's performances (see Table 1). For example, the radius of curvature, heading angle, and lateral distance step response tests observe the step response of yaw rate, yaw, and lateral distance error. Furthermore, a road track with a clothoid spiral shape prepares the ramp response test conditions.

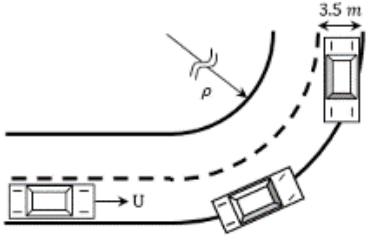

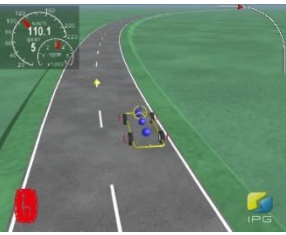
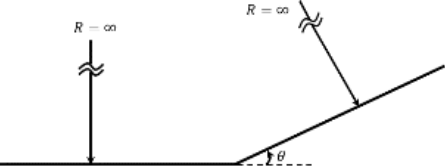
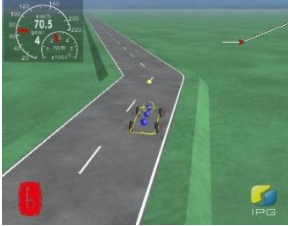

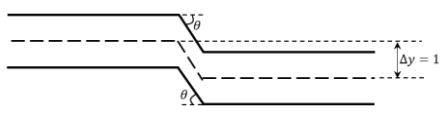


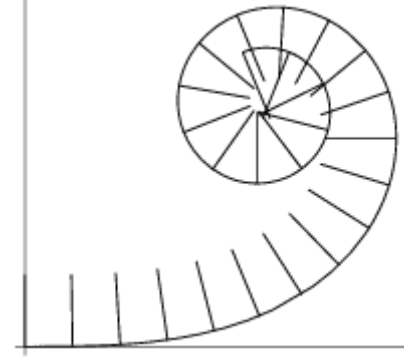
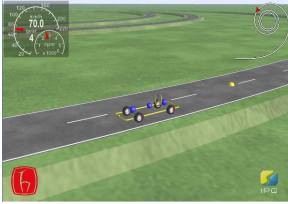

Step response and ramp with the left and right maneuvers examine the performances of controllers and intervention methods. Overall, 8 test scenarios with constant vehicle speed are examined.

#### 3.1. Step Response Maneuver

According to the definition of the step response, a stepwise input is fed into the system. The output can be seen as a nonparametric model of the process. In order to obtain the desired step response, a set of meaningful parameters was chosen to define the behavior of the response. The most commonly chosen parameters of a typical step response for a second-order system with complex poles and no finite zeros are shown in Figure 8:

- Rise Time ( $t_r$ ) - the time it takes for the output to go from 10% to 90% of the final value.
- Peak Time ( $t_p$ ) - the time it takes for the output to reach its maximum value.
- Overshoot -  $(\text{max value} - \text{final value})/\text{final value} \times 100$ .
- Settling Time ( $t_s$ )- The time it takes for the signal to be bounded to within a tolerance of x% of the steady state value.
- Steady State Error ( $e_{ss}$ ) - The difference between the input step value (dashed line) and the final value.

Table 1. Maneuvers used in experiments

Step Response Tests	Step	a) Left	b) Right
 <p>Constant Curvature Step</p>	$\Delta\psi$		
 <p>Angle Step</p>	$\Delta\psi$		
 <p>Lateral Distance Step</p>	$\Delta y$		
<p>Ramp (Clothoid) Test</p>	<p>Ramp</p>	<p>a) Left</p>	<p>b) Right</p>
	$\Delta\psi$		

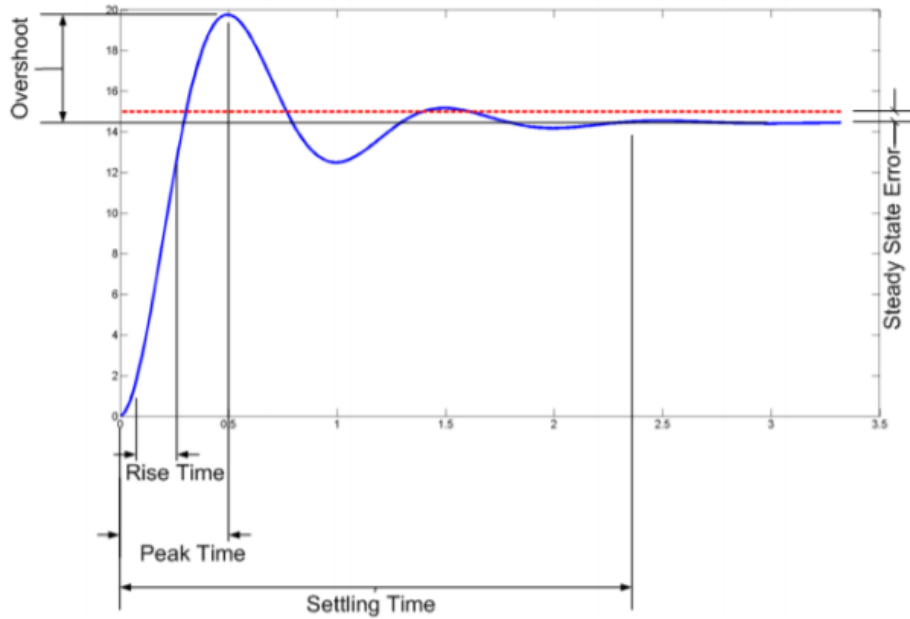


Figure 8. A typical step response diagram

If the system contains no complex poles, the response will not be oscillatory; hence, the peak time and overshoot will not be relevant. Typically, when designing a control system, we will be asked to achieve specific targets for these parameters. For example, in this thesis, a suitable controller was designed such that the rise time is less than 3 seconds and a steady state error of 0.2 meters. These targets will force the vehicle to get back to its lane in less than 3 seconds and finally travel in its lane and track the lane center precisely. It is necessary to either run a simulation and measure the parameters from the step response directly or to define expressions for the parameters in terms of the transfer function coefficients.

In this study, three types of step response maneuvers were designed and examined as below:

- Yaw rate step response ( $\Delta\dot{\psi}$ ) – Constant Curvature
- Yaw step response ( $\Delta\psi$ ) – Angle change
- Lateral distance step response ( $\Delta y$ ) – Lateral Change

The maneuvers were tested with simulations prepared in Matlab-Simulink and CarMaker environments.

### 3.1.1. Constant Curvature Step Test

The radius of curvature is infinite for a straight path, and as the radius value decreases, the curvature becomes sharper. The constant curvature radius was set to 400, as discussed in the Road Model chapter.

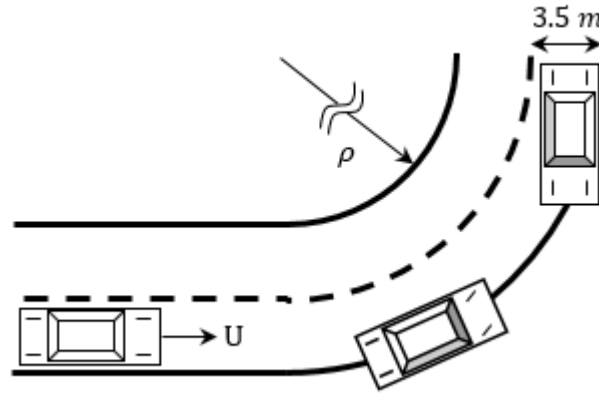


Figure 9. The constant radius of curvature maneuver schematic

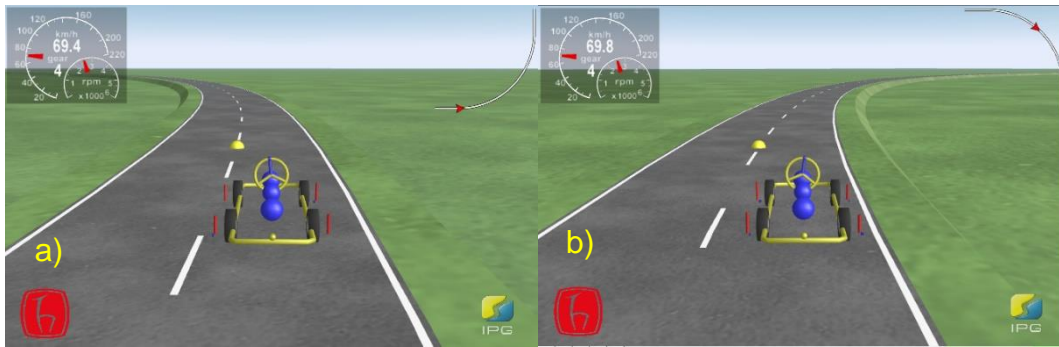


Figure 10. The constant radius of curvature maneuver in CarMaker: **a)** Left, **b)** Right

### 3.1.2. Angle Step Test

As shown in Figure 11 and Figure 12, the vehicle passes from the first straight road to the second straight road, which is connected with the angle of  $\theta$ . To be more precise, if the vehicle direction is  $\psi_{vehicle}$  and the road direction is  $\psi_{road}$ , the difference  $\Delta\psi$  is defined as  $\psi_{vehicle} - \psi_{road}$ . First, the vehicle travels with the same direction as the road, and the yaw angle difference is zero ( $\Delta\psi = 0$ ). Next, the vehicle reaches the angle change point,  $\psi_{vehicle}$  remains zero and  $\psi_{road}$  suddenly becomes  $\theta$ , so the yaw angle difference becomes  $\Delta\psi = \theta$ . After this sudden change, the expected controller behavior is that it steers the vehicle back to the new lane path.

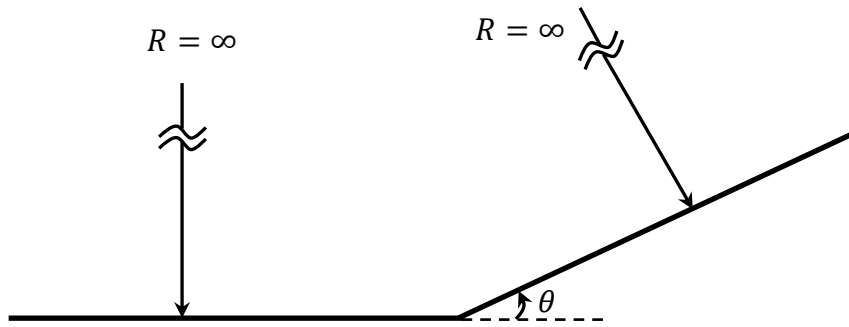


Figure 11. Angle step maneuver schematic

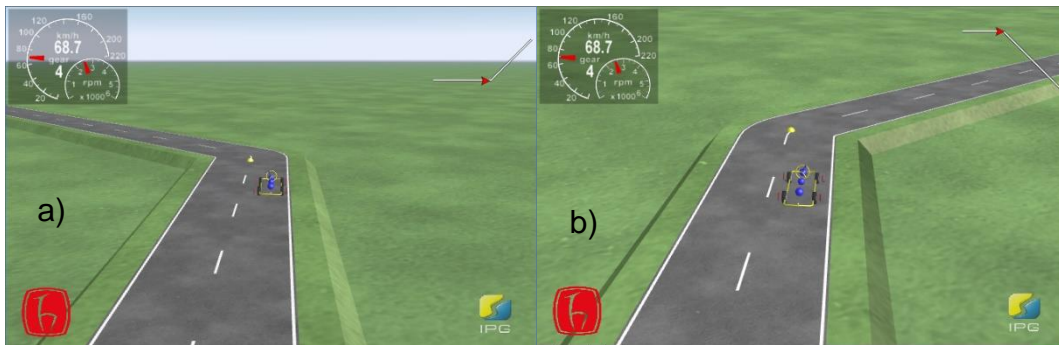


Figure 12. Angle step maneuver in CarMaker: a) Left, b) Right

### 3.1.3. Lateral Distance Step Test

In this section, the vehicle passes from a straight road to a second straight road connected at a certain  $\Delta y$  lateral distance (See Figure 13 & Figure 14). The vehicle follows the lane center of the road; in this case, the lateral distance difference is zero ( $\Delta y = 0$ ). At the sudden lateral lane change point, the lateral distance becomes  $\Delta y = 1$  m. From this point on, the controller activates and reduces the lateral distance difference to zero.

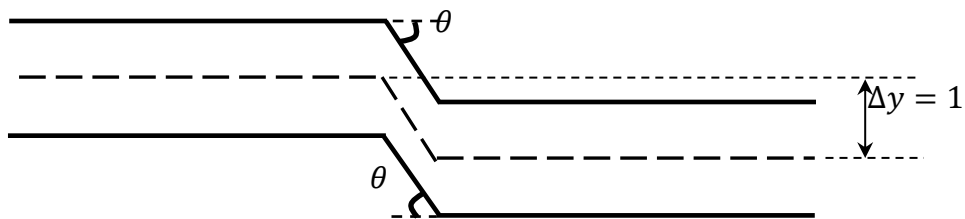


Figure 13. Lateral distance step maneuver schematic



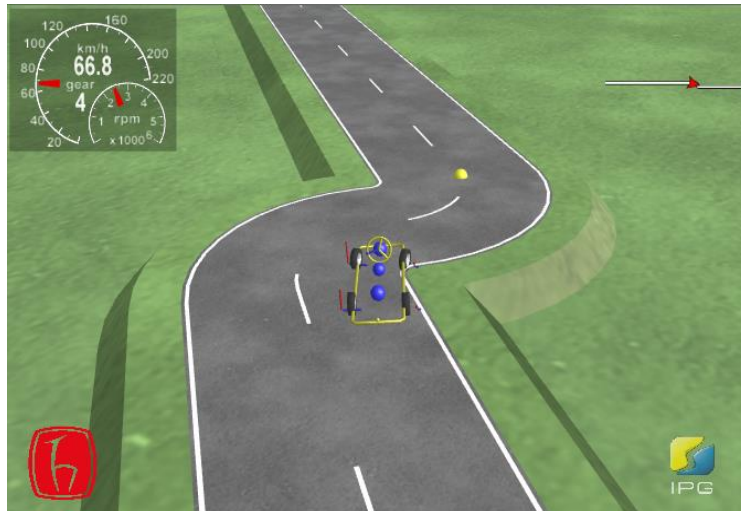


Figure 14. Lateral distance step maneuver schematic in CarMaker

### 3.2. Ramp Response Maneuver

Examining the dynamic performance of lane-keeping configurations and controllers with ramp (Clothoid Spiral) maneuvers can be done by testing the vehicle on a clothoid spiral path. The clothoid spiral path is defined by the radius of curvatures sharpening from start to finish and the total angle of the path. From a bird's eye view, it has a road profile that resembles a spiral shape with a continuously decreasing radius of curvature. This experiment aims to perform the ramp response of the radius of curvature of the road (yaw rate ramp response) and to examine the system's limits.

### 3.3. Conclusion

The importance and originality of this study is that it explores extraordinary scenarios for testing the performance of novel intervention method. For example, the Step response and ramp considering left and right maneuvers provide 8 test scenarios.

The next chapter demonstrates the tests performed to examine the performance of intervention configurations and controller methods. The LQR and MPC controllers provide the steering and braking inputs for controlling the vehicle according to the conditions of the test scenarios and intervention configuration.

## 4. RESULTS AND DISCUSSION

### 4.1. Intervention Configurations Performance

The present study fills a gap in the literature by undertaking the performance of only Braking (B), Only Steering (S), and Coordinated Braking and Steering (S+B). First, the LQR controller provides the input for examining intervention configurations' step response performances. Then, the results demonstrate that coordinated configuration (S+B) has the best performance. Finally, since the novel controller provided the best performance, the tests were repeated for MPC with these values and compared with the LQR results.

#### 4.1.1. Constant Curvature Step Test

In this section, experiments were carried out with a constant radius of curvature, as shown in Figure 9 and Figure 10.

Maximum overshoot ( $M_{os}$ ) and response time ( $t_{os}$ ) values of control inputs are given in Table 2. According to the results obtained here, the (S+B) configuration method had a faster response time than the other two methods (See Figure 15) and required lower control input (See Figure 16). The (S+B) configuration utilizes the force potential of three wheels and two actuators in a coordinated manner, while the (S) and (B) methods utilize the potential of two wheels. According to the results, the (S+B) configuration required 40% less steering input than the (S) method and up to 65% less braking torque input than the (B) method to follow the lane. Taking the same curvature with a lower control input gives the controller an advantage in staying below the maximum control signal value the vehicle can apply. Assuming that the maximum braking torque that the vehicle can apply is 700 Nm and the maximum steering angle is 15 degrees, it is clear that the other two methods are ineffective in sharper curvatures as they reach their performance limits (See Figure 15). On the other hand, even if one of the control signals reaches its maximum value, the other control signal can control the vehicle though (S+B) method becomes a safer control method, especially in sharp curves or maneuvers with high yaw angle values.

Table 2. Constant Curvature Step Test, Controller input performance ( $\rho=400m$ ,  $\theta=90^\circ$ ,  $U=19.45$  m/s)

Control Input	Intervention Configuration	Left		Right	
		$t_{os}$ [s]	$M_{os}$	$t_{os}$ [s]	$M_{os}$
Steering	(S)	3,741	11.46°	3,754	11.57°
	(S + B)	2,452	6.349°	2,451	6.399°
Brake	(B)	3,317	684Nm	3,788	689,119Nm
	(S + B)	2,668	239,2Nm	3,169	241,883Nm

Table 3. Constant Curvature Step Test, Error, and model output performance ( $\rho=400m$ ,  $\theta=90^\circ$ ,  $U=19.45$  m/s)

Error	Intervention Configuration	Left			Right		
		$t_{os}$ [s]	$M_{os}$	$t_{s(0.05)}$ [s]	$t_{os}$ [s]	$M_{os}$	$t_{s(0.05)}$ [s]
$(\Delta y)$	(B)	3,2	1,44m	24,37	3,151	1,451m	24,314
	(S)	3,63	0,983m	14,62	3,534	1m	14,544
	(S + B)	2,687	0,394m	8,2	2,576	0,4m	8,164
$(\Delta \psi)$	(B)	1,937	3.457°	26,546	1,935	3,476°	22,916
	(S)	2,116	2.882°	16,616	2,1	2,901°	16,646
	(S + B)	1,562	2.222°	7,016	1,589	2,235°	7,036
$(\dot{\Delta \psi})$	(B)	0.185	2.901°/s	24.362	0.1	2.822°/s	18.632
	(S)	0.101	2.822°/s	18.462	0.184	2.902°/s	24.372
	(S + B)	0.132	2.856°/s	11.332	0.128	2.856°/s	8,042

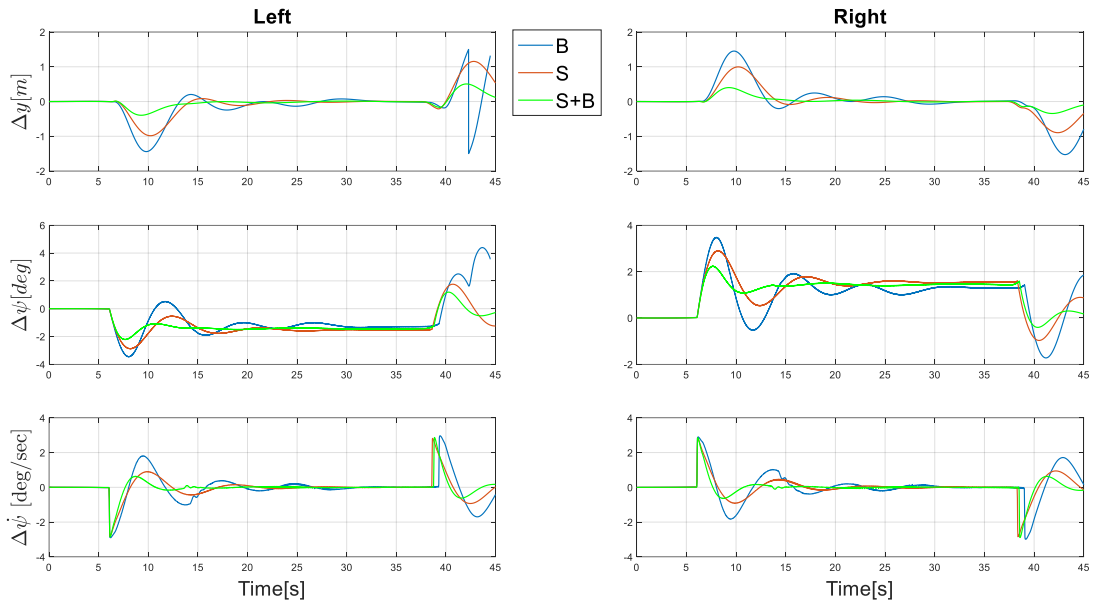


Figure 15. Constant Curvature Step Test, Intervention configurations error

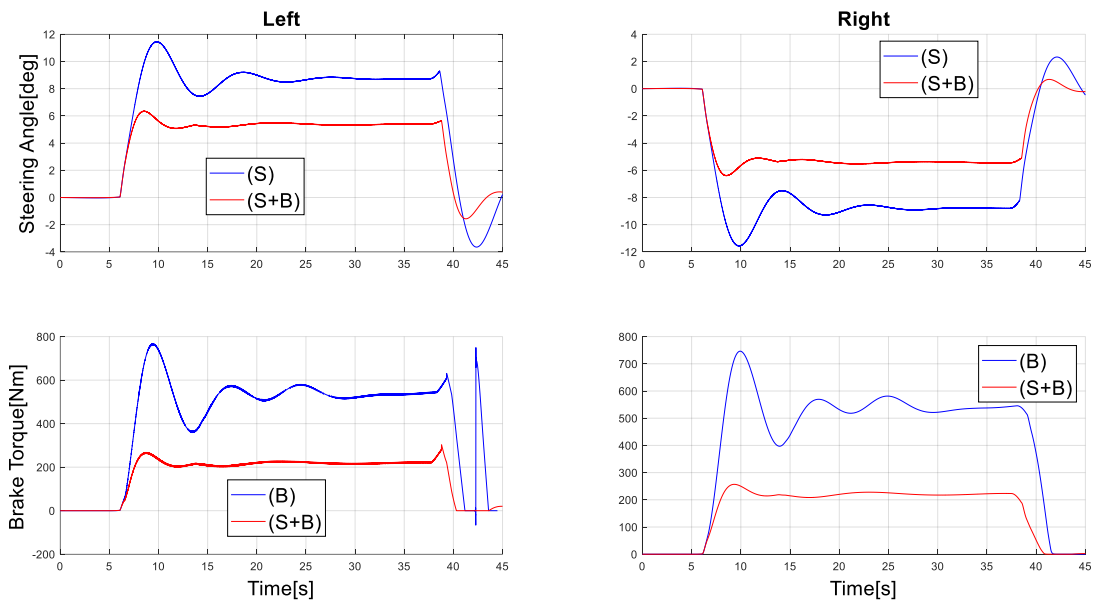


Figure 16. Constant Curvature Step Test, Intervention configurations, controller input

Table 3 examines the error and model output performances. Table values show that the (S + B) method has a faster response time ( $t_{os}$ ) and settling time ( $t_s$ ) than other methods. The (S + B) had a faster settling time than (S) by at least 7 seconds and the (B) method by at least 16 seconds. Settling time represents the vehicle's duration on the opposite lane or shoulder. The proposed (S + B) configuration can potentially prevent accidents in the event of unintended lane departure by maximally reducing lateral distance error and settling time.

### 4.1.2. Angle Step Test

In the angle step response test, lane tracking becomes more difficult as the angle value increases. Therefore, the step angle experiments started from five degrees and increased by five degrees. The angle at which lane protection could not be provided was determined. The most significant integer yaw angle ( $\theta$ ) was obtained by reducing this angle by one degree. This angle was the best performance point of the tested configuration. The step angle's geometric maneuver shape requires a minimum curvature radius. Due to the path radius limit of the IPG CarMaker software, the radius of curvature was chosen as four meters ( $R=4$ ).

The intervention configurations were examined, and maximum angle values with the successful intervention were determined. The (B) configuration with  $8^\circ$  to the left and  $9^\circ$  to the right had the lowest performance, the (S) method with  $14^\circ$  to the left and  $10^\circ$  to the right had medium performance, and the SB method with  $22^\circ$  to the left and right had the best performance (See Figure 17).

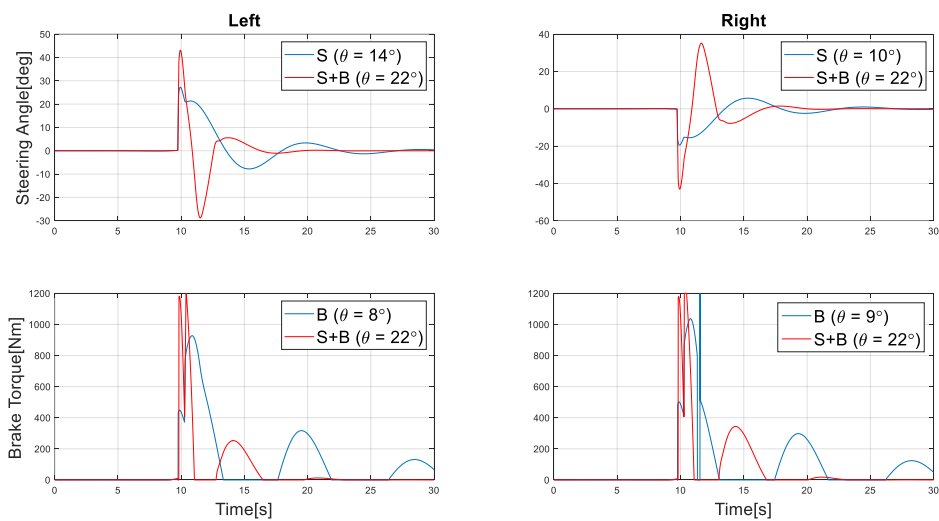


Figure 17. Angle Step Test, Intervention configurations, controller input

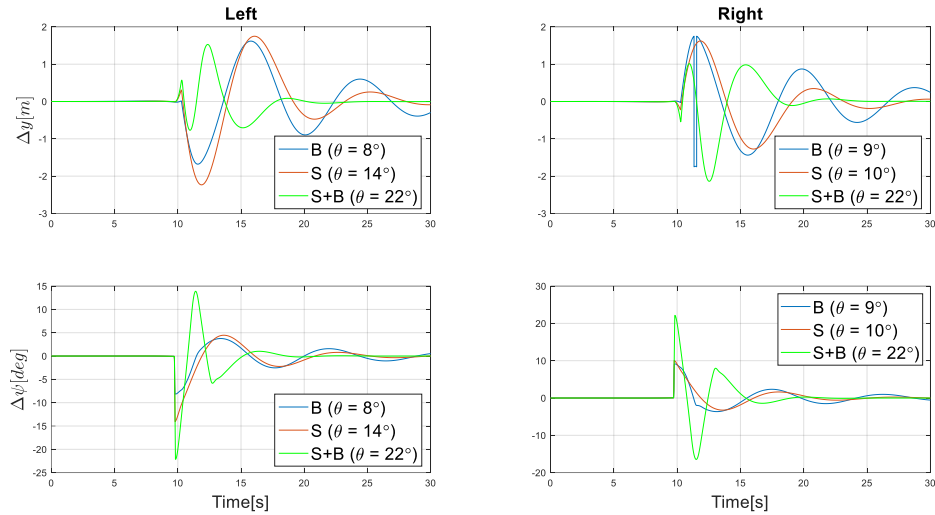


Figure 18. Angle Step Test, Intervention configurations error

Table 4 presents the control inputs performance of the angle step response, testing at the performance limit of each configuration. The (S+B) configuration provided a more than 55% yaw angle performance with a 16-degree steering angle difference compared to the (S) method. Comparing the (S+B) configuration to the (B) method provided 145% better yaw angle control with almost the same braking torque input.

The performance metrics in Table 5 show that the (S+B) configuration has the lowest lateral distance error deviation value. However, (S+B) exhibits a better yaw angle control performance of 8 and 14 degrees compared to (S) and (D) methods, respectively (See Figure 18).

Table 4. Angle Step Test, Controller input performance (U=19.45 m/s)

Control Input	Intervention Configuration	Left			Right		
		$t_{os}$ [s]	$M_{os}$	$\theta$ [°]	$t_{os}$ [s]	$M_{os}$	$\theta$ [°]
Steering	(S)	0.202	27.26°	14	0.192	19.48°	10
	(S + B)	0.203	43.09°	22	0.203	43.06°	22
Brake	(B)	1.139	927.6Nm	8	1.014	1037Nm	9
	(S + B)	0.117	1181Nm	22	0.036	1179Nm	22

Table 5. Angle Step Test, Error, and model output performance (U=19.45 m/s)

Error	Intervention Configuration	Left			Right		
		$t_{os}$ [s]	$M_{os}$	$\theta$ [°]	$t_{os}$ [s]	$M_{os}$	$\theta$ [°]
$(\Delta y)$	(B)	1.849	1.678m	8	1.617	1.75	9
	(S)	2.149	2.233m	14	2.107	1.623	10
	(S + B)	2.637	1.529m	22	2.807	2.138	22
$(\Delta\psi)$	(B)	0.095	8.146°	8	0.095	9.146	9
	(S)	0.052	14.04°	14	0.035	10.04	10
	(S + B)	0.178	21.465°	22	0.081	22.14	22

#### 4.1.3. Lateral Distance Step Test

The lateral distance step response test consists of two parallel roads with a lateral distance of  $\Delta y = 1$  m between the two road segments and a junction (junction angle  $\theta$ , and radius  $R$ ).

The maximum overshoot values of the control inputs are similar to each other for different scenarios (see Table 6). The reason is, in the tests, only the junction angle of the two-track roads and the radius of curvature were selected within the software limits, the lateral distance was defined as one meter, and the step response test was prepared with different transition times.

The overshoot ( $M_{os}$ ) values of the lateral distance error obtained in the tests are given in Table 7. Overshoot distance ( $X_{os}$ ) and settling distance ( $X_{s(0.05)}$ ) parameters are examined instead of overshoot time ( $t_{os}$ ) and settling time ( $t_{s(0.05)}$ ) (See Figure 19). According to the test metrics given in the table, the (S+B) method overshoot values were 10% less than the (S) method and less than 50% according to the (B) method. According to the results, the (S+B) method has approximately 150 meters less settling distance than the (S) method. Method (B), on the other hand, does not seem to have a settlement process in the time frame used in the test. The fastest settling time in all tests was achieved by the (S+B) configuration, which is one of the most critical factors in preventing cross-lane crashes. The vehicle passes the lateral junction segment of the Road in about 0.15 seconds. The angle and yaw rate differences cause an overshoot in the first 0.5 seconds of the test.

Table 6. Lateral Distance Step Test, Controller input performance (U=19.45 m/s)

Test	Control Input	Intervention Configuration	Left		Right	
			$t_{os}$ [s]	$M_{os}$	$t_{os}$ [s]	$M_{os}$
$R = 4m$ $\theta = 28.96^\circ$	Steering	(S)	0.104	50.55°	0.104	50.56°
		(S + B)	0.105	50.04°	0.105	50.04°
	Brake	(B)	0.02	1178Nm	0.02	1178Nm
		(S + B)	0.02	1175Nm	0.02	1175Nm
$R = 5$ $\theta = 25.84^\circ$	Steering	(S)	0.116	45.49°	0.116	45.49°
		(S + B)	0.117	45.03°	0.117	45.03°
	Brake	(B)	0.01	1167Nm	0.01	1167Nm
		(S + B)	0.02	1165Nm	0.02	1165Nm
$R = 10$ $\theta = 18.19^\circ$	Steering	(S)	0.167	32.51°	0.167	32.51°
		(S + B)	0.168	32.48°	0.168	32.48°
	Brake	(B)	0.01	1182Nm	0.01	1182Nm
		(S + B)	0.02	1178Nm	0.02	1178Nm

Table 7. Lateral Distance Step Test, Error, and model output performance (U=19.45 m/s)

Test	Intervention Configuration	Left ( $\Delta y$ )			Right ( $\Delta y$ )		
		$X_{os}$ [m]	$M_{os}$ [m]	$X_{s(0.05)}$ [m]	$X_{os}$ [m]	$M_{os}$ [m]	$X_{s(0.05)}$ [m]
$R = 4m$ $\theta = 28.96^\circ$	(B)	75,5	0,713	> 500	75,1	0,714	> 500
	(S)	63,7	0,342	255,1	63	0,352	255,8
	(S + B)	48	0,225	82,9	47,1	0,234	81,8
$R = 5$ $\theta = 25.84^\circ$	(B)	74,5	0,696	> 500	73,5	0,697	> 500
	(S)	64	0,341	254,9	64,3	0,35	255,8
	(S + B)	47,3	0,223	81	45,6	0,231	109,6
$R = 10$ $\theta = 18.19^\circ$	(B)	69,7	0,626	> 500	69,4	0,629	> 500
	(S)	64	0,341	254,9	63,5	0,347	255
	(S + B)	44	0,213	127	42,9	0,22	127,7



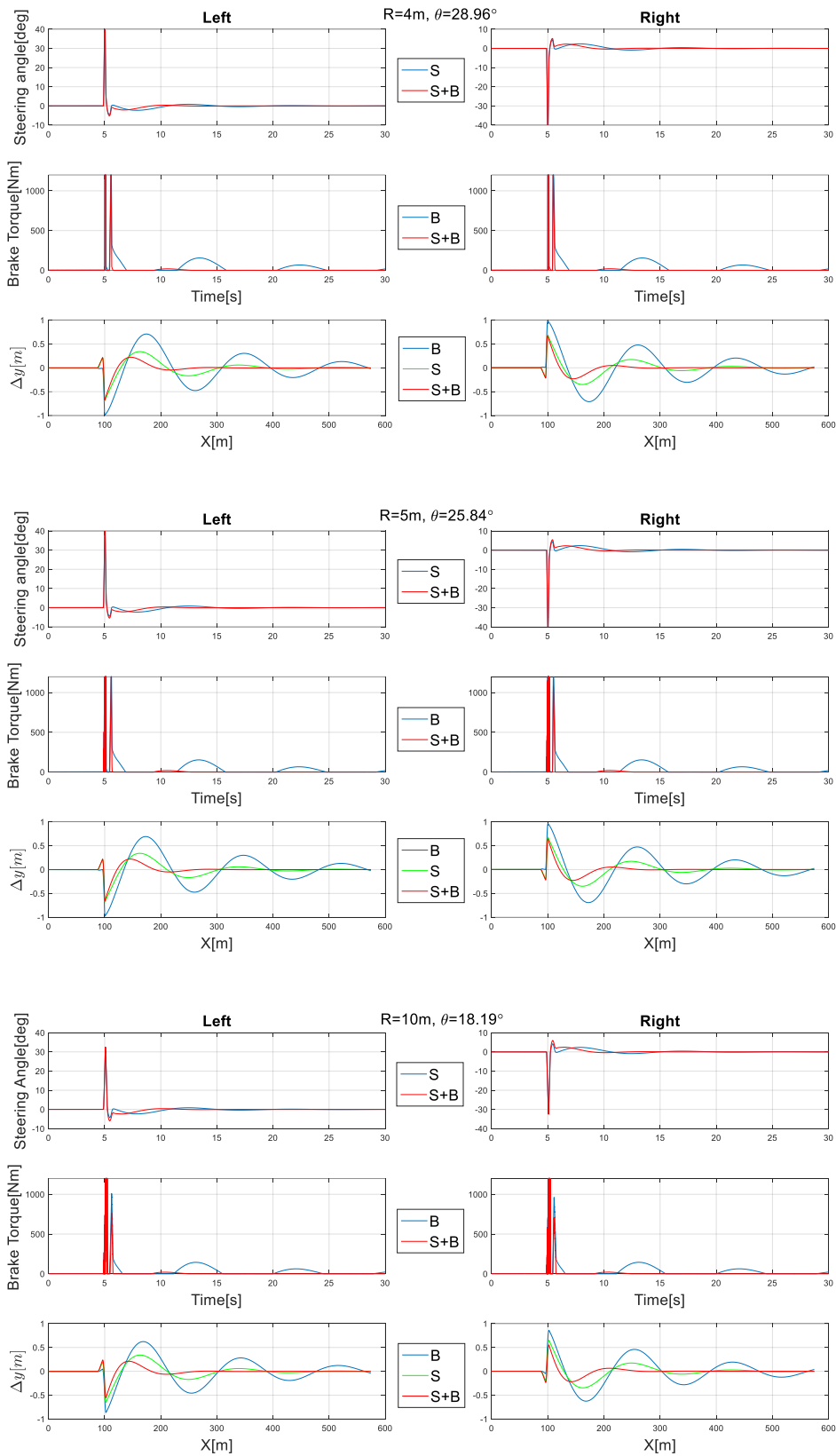


Figure 19. Lateral Distance Step Test, Control Inputs, and performances

## 4.2. Controllers Performance

This chapter describes and discusses the performance comparison of LQR and MPC controllers. As mentioned in the “Interventions configurations performance” chapter, the coordinated Steering and Braking (S+B) configuration performs best. Therefore, this chapter compares the performance of the (S+B) configuration with LQR and MPC controllers.

### 4.2.1. Constant Curvature Step Test

In this section, as shown in Figure 9 and Figure 10, experiments were carried out with a constant radius of curvature.

Table 8. Constant Curvature Step Test of LQR and MPC controllers, Controller input performance ( $\rho=400m$ ,  $\theta=90^\circ$ ,  $U=19.45$  m/s)

Control Input	Intervention Configuration	Left		Right	
		$t_{os}$ [s]	$M_{os}$	$t_{os}$ [s]	$M_{os}$
Steering	MPC (S + B)	2.148	5.490°	1.984	5.537°
	LQR (S + B)	2.452	6.349°	2.451	6.399°
Brake	MPC (S + B)	–	~250Nm	–	~250Nm
	LQR (S + B)	2.668	239.2Nm	3.169	241.883Nm

Table 9. Constant Curvature Step Test of LQR and MPC controllers, Error, and model output performance ( $\rho=400m$ ,  $\theta=90^\circ$ ,  $U=19.45$  m/s)

Error	Intervention Configuration	Left			Right		
		$t_{os}$ [s]	$M_{os}$	$t_{s(0.05)}$ [s]	$t_{os}$ [s]	$M_{os}$	$t_{s(0.05)}$ [s]
$(\Delta y)$	MPC (S + B)	2.411	0.069	2.431	2.289	0.071	2.298
	LQR (S + B)	2.687	0.394m	8.2	2.576	0.4m	8.164
$(\Delta \psi)$	MPC (S + B)	1.372	1.804°	3.136	1.378	1.810°	3.169
	LQR (D + F)	1.562	2.222°	7.016	1.589	2.235°	7.036
$(\Delta \dot{\psi})$	MPC (S + B)	0.092	2.867°/s	3.557	0.184	2.876°/s	3.569
	LQR (D + F)	0.132	2.856°/s	11.332	0.128	2.856°/s	8.042

Maximum overshoot ( $M_{os}$ ) and response time ( $t_{os}$ ) values of control inputs are given in Table 8. According to the results, the MPC method had a faster response time than the LQR (See Figure 20) and required lower control input (See Figure 21). According to the

results, the MPC required 10% less steering input than the LQR method, and there was no braking torque overshoot. In addition, the MPC smoothly controls only one-side brake input despite the LQR method's intervention on both sides. Figure 22 represents the velocities and lateral acceleration of the vehicle, and the MPC performs better than LQR.

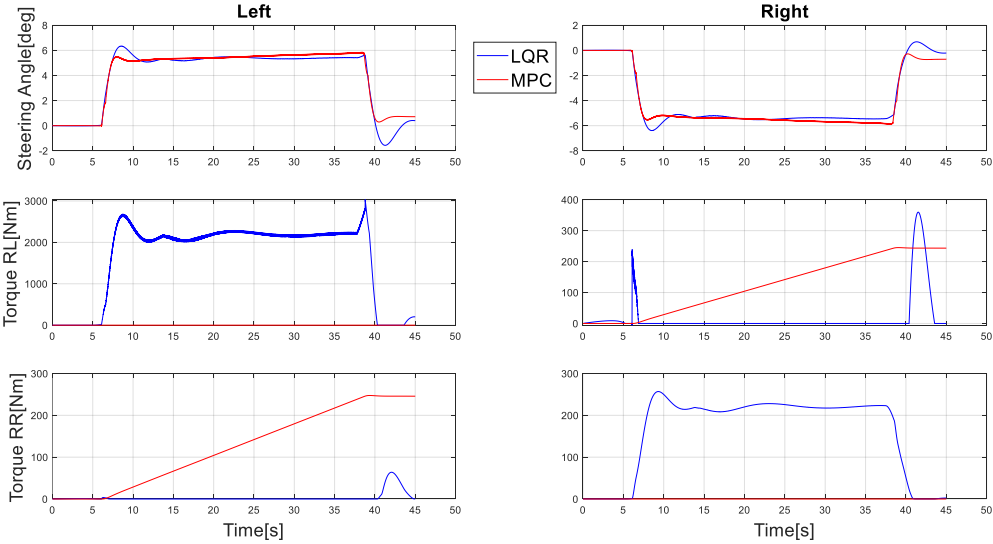


Figure 20. Constant Curvature Step Test of LQR and MPC controllers, Intervention configurations error

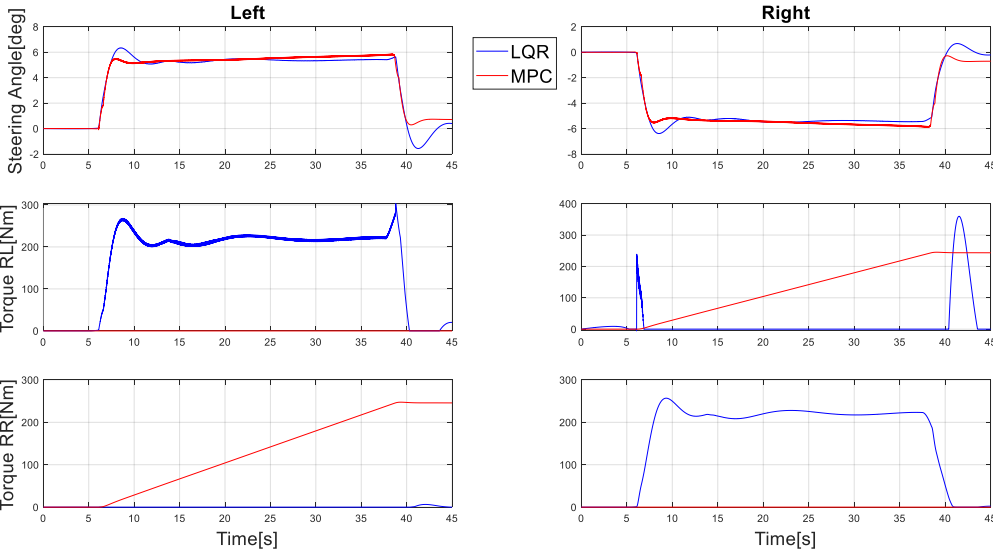


Figure 21. Constant Curvature Step Test of LQR and MPC controllers, control input

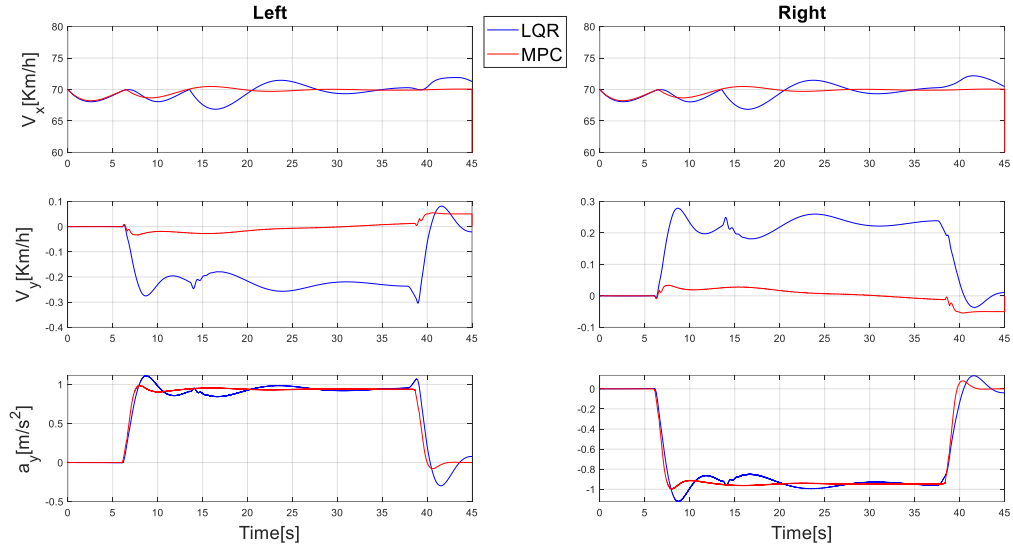


Figure 22. Constant Curvature Step Test of LQR and MPC controllers, velocities, and acceleration

Table 9 examines the error and model output performances. Table values show that the MPC method has a faster response time ( $t_{os}$ ) and settling time ( $t_s$ ) than LQR. The major difference is that settling time is faster by at least 3.5 seconds.

#### 4.2.2. Angle Step Test

In the angle step response test, lane tracking becomes more difficult as the angle value increases. Therefore, the intervention configurations were examined, and maximum angle values with the successful intervention were determined. The MPC configuration with  $26^\circ$  to the left and right had the best performance, and the LQR method with  $22^\circ$  to the left and right had the lowest performance, so  $22^\circ$  is selected as the test limit (See Figure 23).

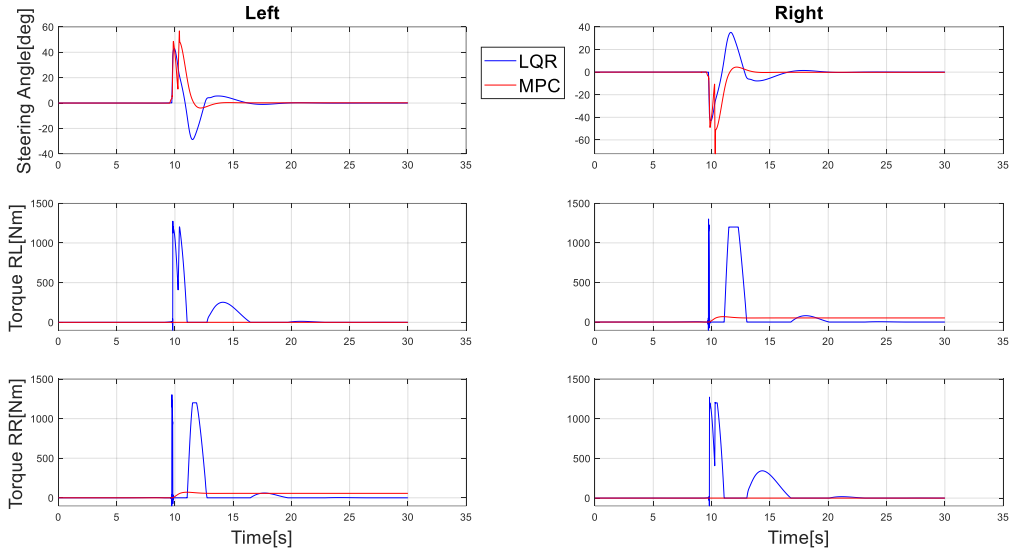


Figure 23. Angle Step Test of LQR and MPC controllers, controller input

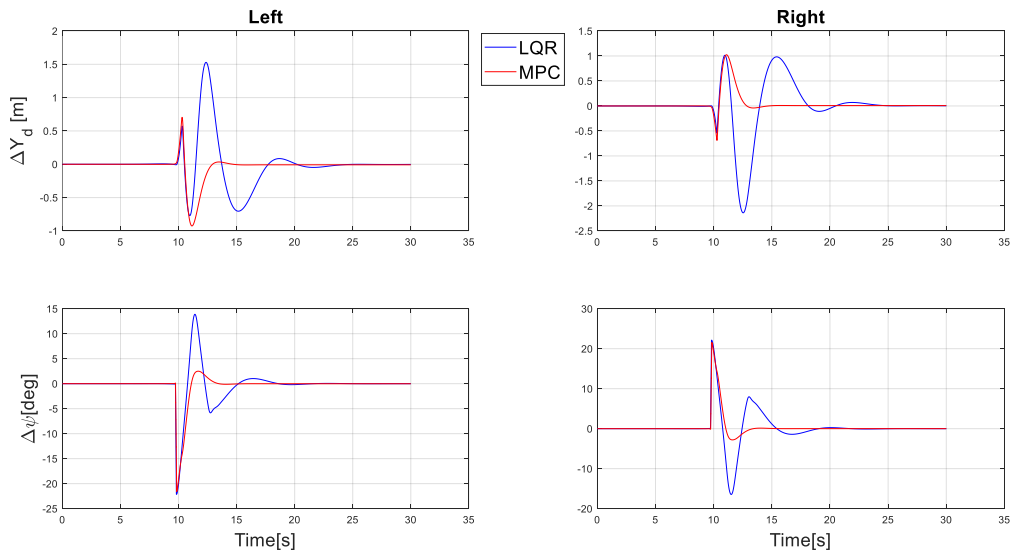


Figure 24. Angle Step Test of LQR and MPC controllers, yaw and lateral distance error

Table 10 presents the control inputs performance of the angle step response, testing at the performance limit of LQR. Again, the MPC provided the lowest braking torque values, which increases the ability to perform better response at severe maneuvers.

The performance metrics in Table 11 show that the MPC has the lowest lateral distance error deviation value and settling time (See Figure 24).

Table 10. Angle Step Test of LQR and MPC controllers, Controller input performance (U=19.45 m/s,  $\theta = 22^\circ$ )

Control Input	Intervention Configuration	Left		Right	
		$t_{os}$ [s]	$M_{os}$	$t_{os}$ [s]	$M_{os}$
Steering	MPC (S + B)	0.116	46.56°	0.115	46.75°
	LQR (S + B)	0.203	43.09°	0.203	43.06°
Brake	MPC (S + B)	0.942	66Nm	0.884	67Nm
	LQR (S + B)	0.117	1181Nm	0.036	1179Nm

Table 11. Angle Step Test of LQR and MPC controllers, Error and model output performance (U=19.45 m/s,  $\theta = 22^\circ$ )

Error	Intervention Configuration	Left			Right		
		$t_{os}$ [s]	$M_{os}$	$t_{s(0.05)}$ [s]	$t_{os}$ [s]	$M_{os}$	$t_{s(0.05)}$ [s]
$(\Delta y)$	MPC (S + B)	1.318	0.925m	5.166	1.023	1.414	3.933
	LQR (S + B)	2.637	1.529m	9.554	2.807	2.138	10.505
$(\Delta\psi)$	MPC (S + B)	0.151	22.145°	3.612	0.072	22.143°	3.647
	LQR (S + B)	0.178	21.465°	7.987	0.081	22.14°	8.487

#### 4.2.3. Lateral Distance Step Test

The lateral distance step response test consists of two parallel roads with a lateral distance of  $\Delta y = 1 \text{ m}$  between the two road segments and a junction (junction angle  $\theta$ , and radius  $R$ ). The maximum overshoot values of the control inputs are similar to each other for different scenarios (see Table 6) with the same controller method (LQR). The reason is, in the tests, only the junction angle of the two-track roads and the radius of curvature were selected within the software limits, the lateral distance was defined as one meter, and the step response test was prepared with different transition times. So in this part ( $R = 10$ ,  $\theta = 18.19^\circ$ ) was selected. The MPC method intervenes with zero braking torque (the LQR intervenes brakes suddenly at about 1100NM) and a six times lower steering angle than the LQR method.

The overshoot ( $M_{os}$ ) values of the lateral distance error obtained in the tests are given in Table 13. Overshoot distance ( $X_{os}$ ) and settling distance ( $X_{s(0.05)}$ ) parameters are

examined instead of overshoot time ( $t_{os}$ ) and settling time ( $t_{s(0.05)}$ ) (See Figure 19). According to the test metrics in the table, the LQR method's overshoot values were 20% less than the MPC method; however, the LQR's second overshoot values are more significant than MPC's overshoot values. The settling time for both control methods is the same. Overall, The MPC has the best performance.

Table 12. Lateral Distance Step Test of LQR and MPC controllers, Controller input performance ( $U=19.45$  m/s,  $R = 10$ ,  $\theta = 18.19^\circ$ )

Control Input	Intervention Configuration	Left		Right	
		$t_{os}$ [s]	$M_{os}$	$t_{os}$ [s]	$M_{os}$
Steering	MPC (S + B)	0.172	5.694°	0.173	5.686°
	LQR (S + B)	0.168	32.48°	0.168	32.48°
Brake	MPC (S + B)	–	0Nm	–	0Nm
	LQR (S + B)	0.02	1178Nm	0.02	1178Nm

Table 13. Lateral Distance Step Test of LQR and MPC controllers, Error and model output performance ( $U=19.45$  m/s,  $R = 10$ ,  $\theta = 18.19^\circ$ )

Error	Intervention Configuration	Left			Right		
		$X_{os}$ [m]	$M_{os}$ [m]	$X_{s(0.05)}$ [m]	$X_{os}$ [m]	$M_{os}$ [m]	$X_{s(0.05)}$ [m]
$\Delta y$	MPC (S + B)	43.452	0.534	126.4	42,59	0.546	126.8
	LQR (S + B)	44	0.213	127	42,9	0,22	127,7

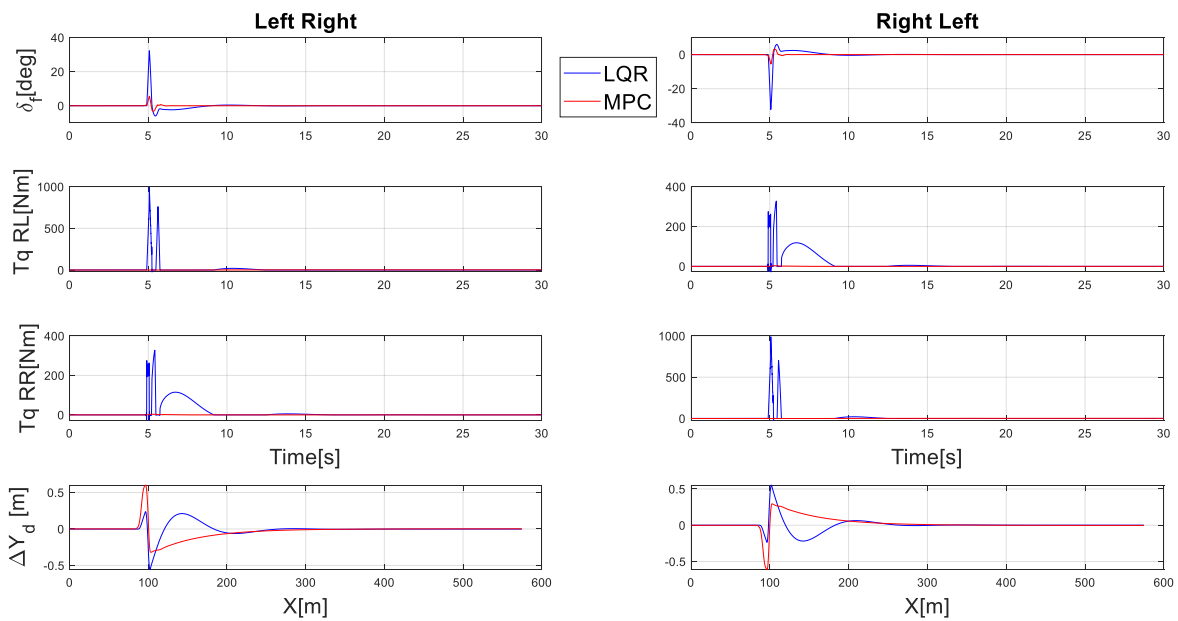


Figure 25. Lateral Distance Step Test of LQR and MPC controllers, Control Inputs, and performances

### 4.3. Ramp Response Maneuver (Clothoid Spiral)

In the clothoid(ramp response) experiment, the road consists of 300 meters straight and about 3500 meters of clothoid path. The radius of curvature of the clothoid road starts from 1000 meters and falls to 100 meters at the end of the path. The total angle of the tracking path is  $6\pi$  (three complete 360-degree rotations). The vehicle speed is 70 km / h.

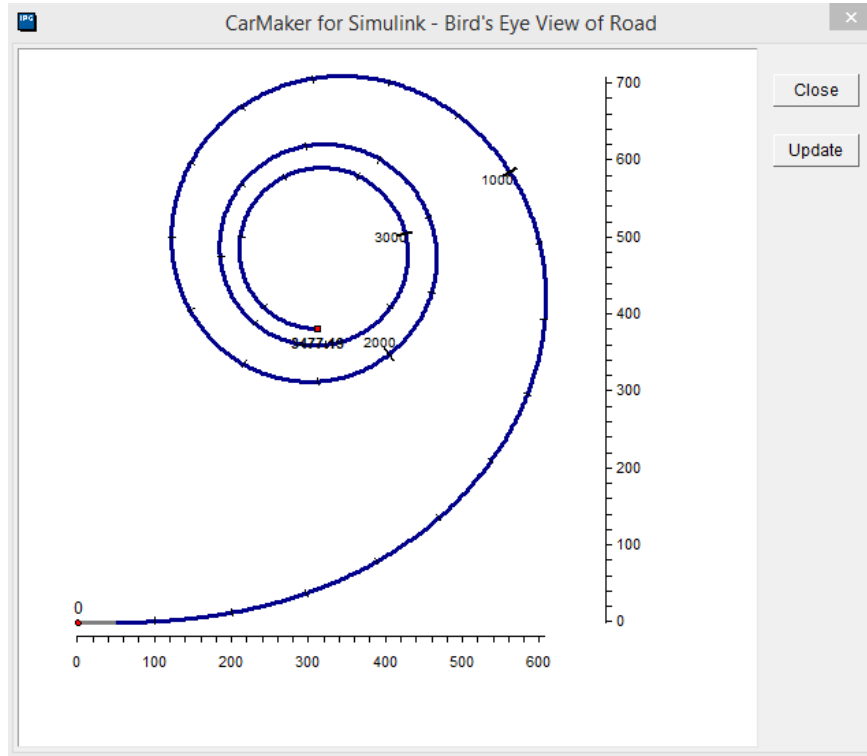


Figure 26. Bird's eye view of the clothoid spiral ramp experiment path

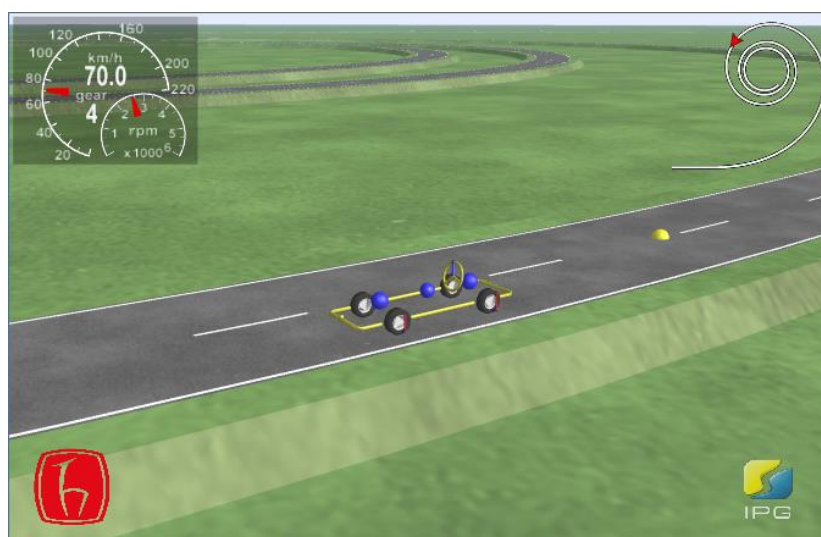


Figure 27. The clothoid spiral ramp experiment path schematic in CarMaker



The results were plotted to see if the two control methods gave the exact measurement. From the data in Figure 29, it is apparent that the LQR controller could not keep the vehicle in its lane at around 120 seconds of the test. Figure 31 demonstrates that this lane crossing happens when the degree of curvature is equal to about 40°. However, the MPC controller could control the vehicle successfully for the degree of curvature of 60, which is about 50% more than the LQR performance.

The degree of curvature is the angle formed by two radii drawn from the circle's center to the ends of a chord 30 meters in length for a given radius. The degree of curvature is a measure of the sharpness of a curve and is approximately calculated by

$$\left( \frac{5729.65}{\text{mean Radius in 30 meters}} \right).$$

In all presented figures, it is visible that the LQR controller inputs oscillate a lot because of continuous changes in disturbance (Radius of Curvature,  $\rho$ ) value.

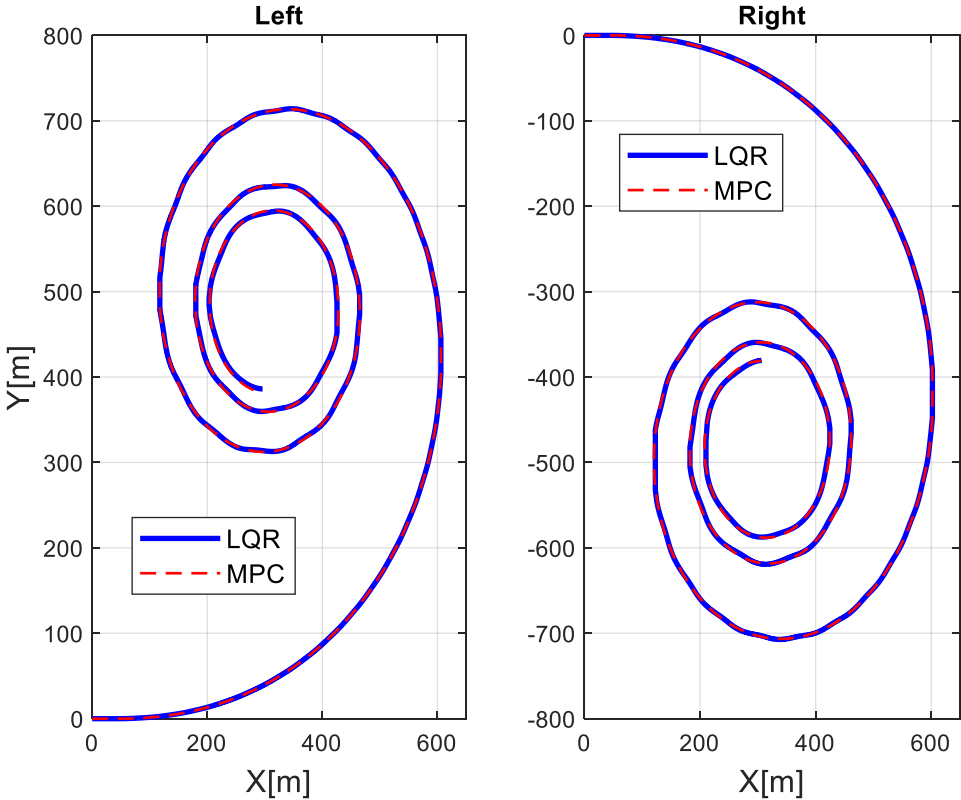


Figure 28. Road and vehicle path, LQR and MPC Lane tracking

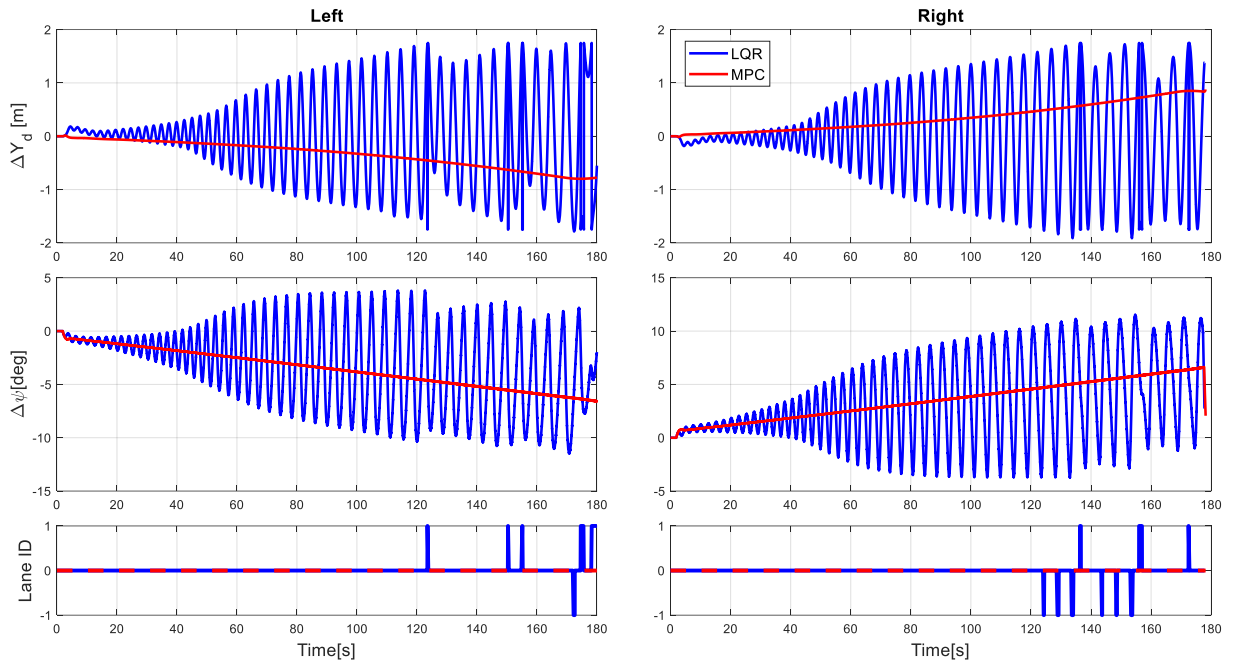


Figure 29. Lateral Distance and Yaw Angle error, Lane ID

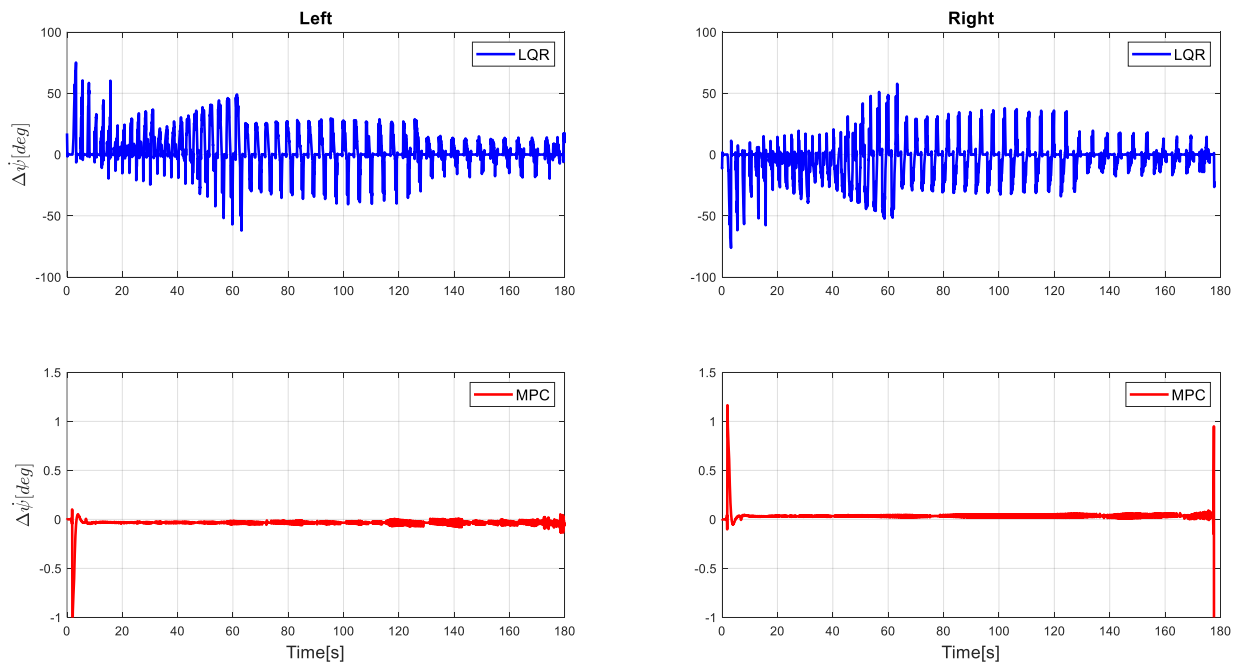


Figure 30. Yaw Rate error distribution during Lane Tracking

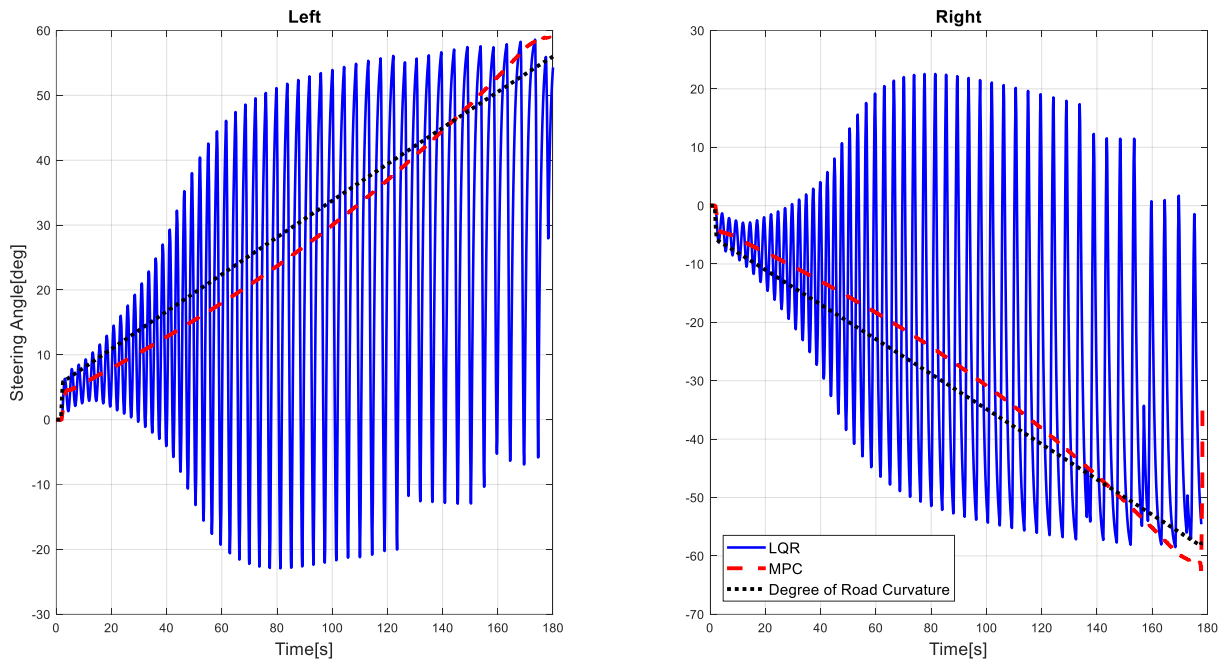


Figure 31. Steering Angle input, degree of road curvature, controller comparison

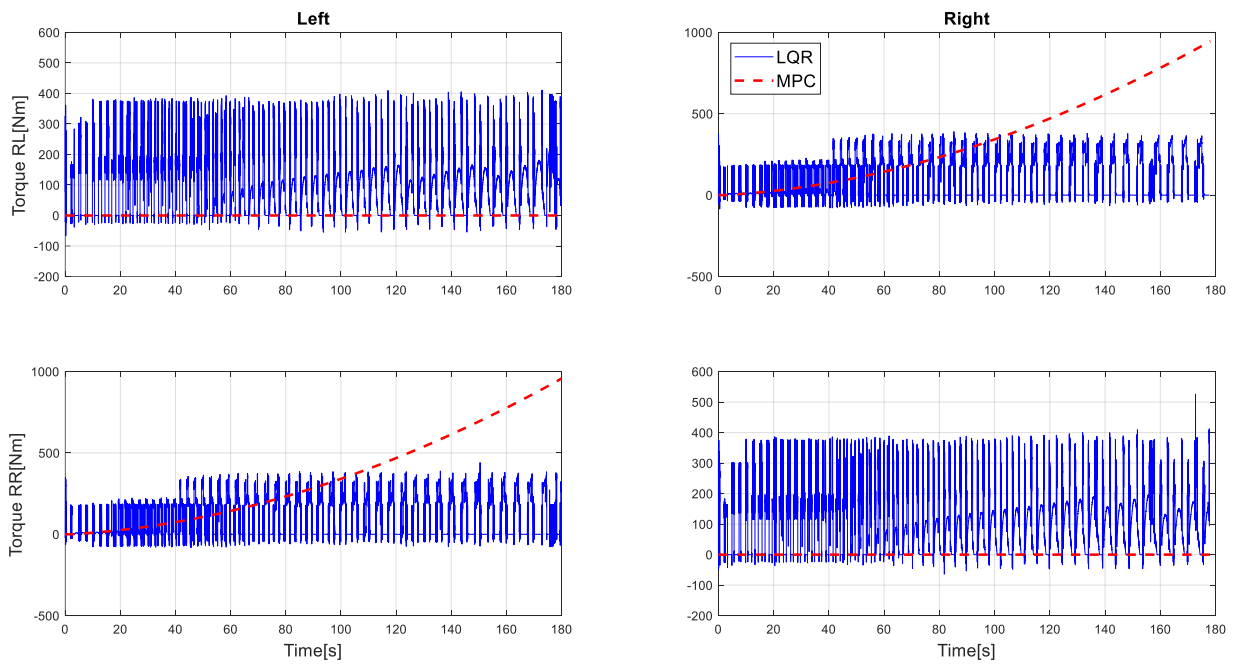


Figure 32. Torque input for Rear Left (RL) and Rear Right (RR)

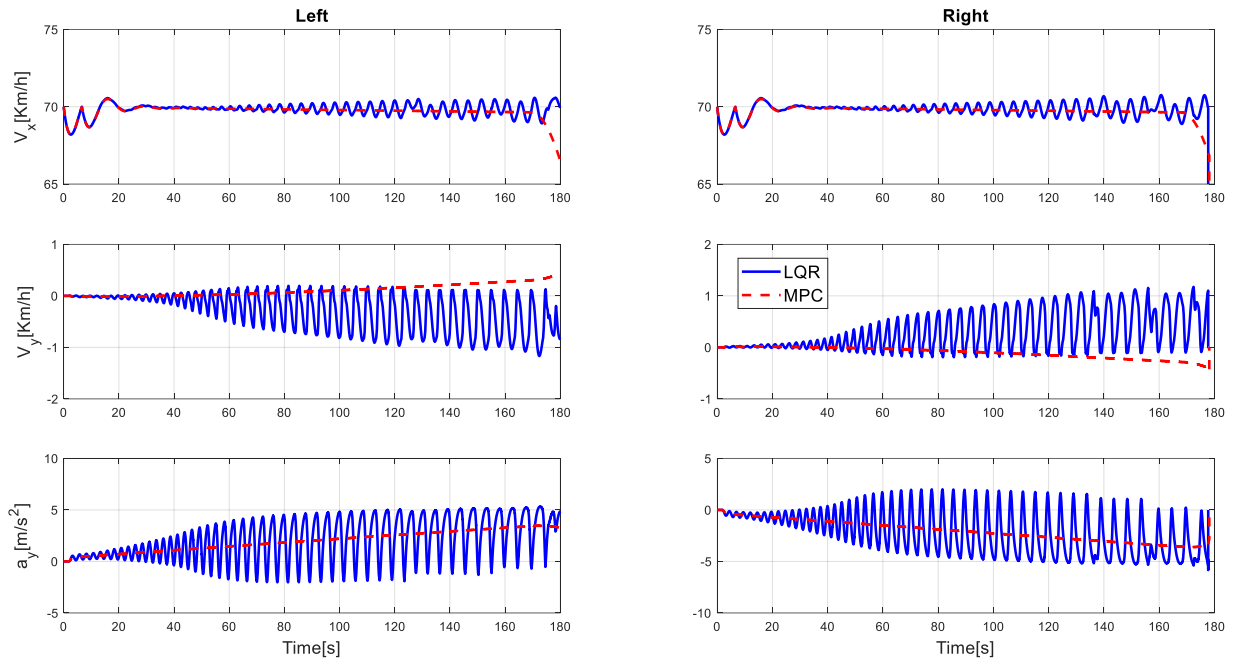


Figure 33. Longitudinal ( $V_x$ ) and Lateral ( $V_y$ ) velocity, Lateral Acceleration ( $a_y$ )

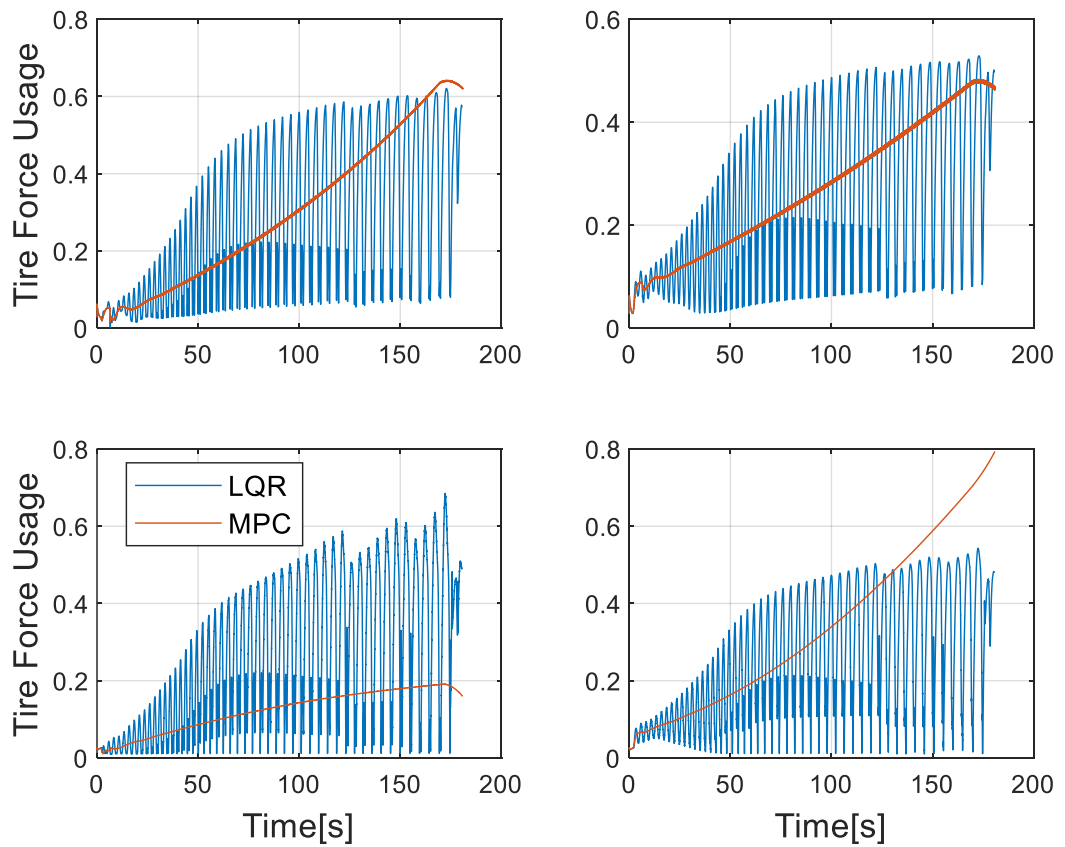


Figure 34. Tire Force Usage, Left Maneuver

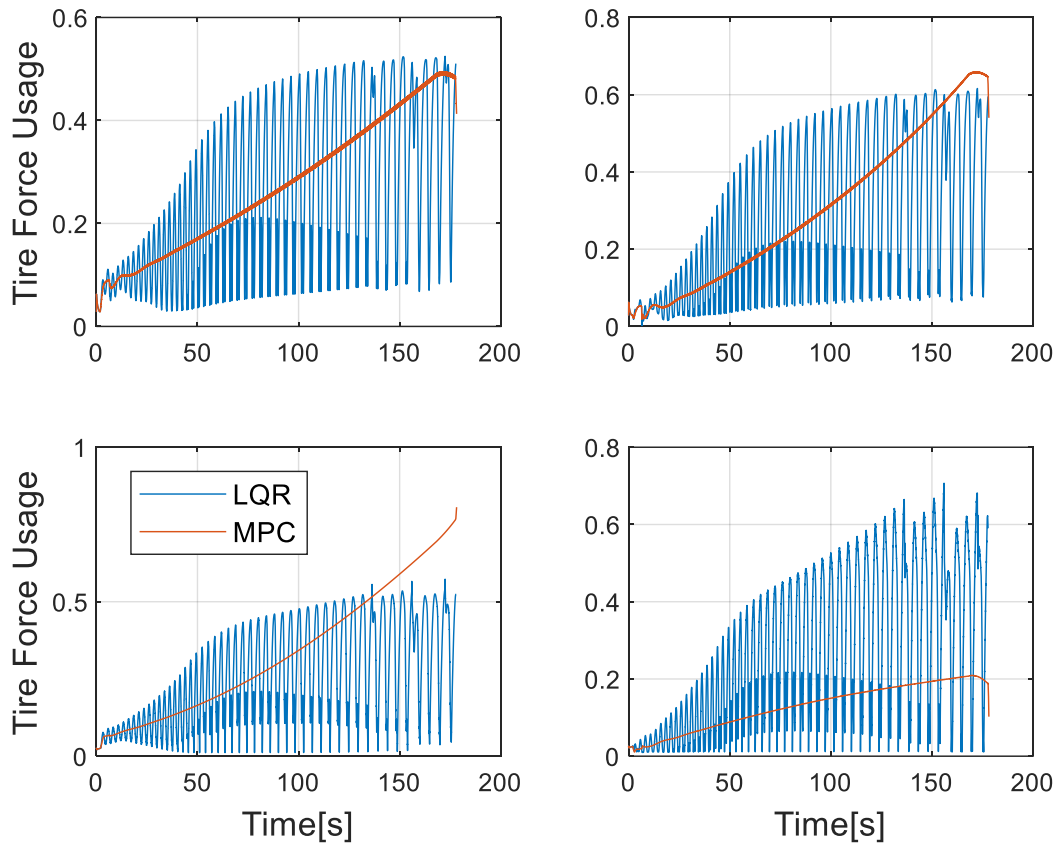


Figure 35. Tire Force Usage, Right Maneuver

#### 4.4. Conclusion

This chapter is divided into two main sections. First is the comparison of intervention configurations. Next is the comparative performance of controller methods.

The simulation results of the constant curvature step test demonstrate that coordinated steering and braking (S+B) configuration required lower control input than the other two methods (only steering (S) and only braking (B)). As a result, this novel intervention configuration (S+B) performs better in analyzing yaw and lateral distance error data. These findings provide solid evidence of at least 16% and at most 34% faster in response speed, at least 37% and at most 73% decrease in maximum error, at least 44% and at most 66% faster in settling time.

It is evidently clear from the Angle step response findings that the (S+B) method provided the best performance compared to other configurations with up to 22 degrees in right and left maneuvers. Unfortunately, the (B) configuration can control the vehicle up to a

maximum of 9 degrees on the right, and the method (S) can control the vehicle up to 14 degrees on the left maneuvers.

These findings prove that the (S+B) required lower control input in lateral distance step simulations than other configurations. Furthermore, it performs at least 20% and at most 37% faster in response speed, at least 33% and at most 68% decrease in maximum error. On the other hand, compared to the (S) controller, the settling time improved by at least 50% and at most 68%. The (B) method does not have a settling time in the time frame used in the simulation. So (S+B) is the winner by a far margin.

The first set of analyses examined the performance of configurations, and results show that coordinated (S+B) has outstanding success. The addition of ramp response simulation follows step response simulations in the controller performance section. The ramp experiment results demonstrate that (S+B), in company with MPC, provides a more robust intervention when the disturbance input of the control model (radius of curvature,  $\rho$ ) rapidly changes. Furthermore, the LQR oscillatory control inputs are evident during the ramp response test. The ramp simulation results demonstrate that the MPC performs about 50% better than the LQR and seldom oscillates.

## 5. CONCLUSION

This study presents a novel intervention configuration that employs coordinated steering and braking action to enhance the performance of the lane assist system. The proposed configuration combines the force potential of the steering and braking systems and allows the vehicle to stay in its lane in severe road curvatures at higher speeds at which either system reaches its actuation limits and cannot control the vehicle when used alone.

The literature survey and market research about available lane-departure assistance systems indicate that steering and braking are the most common intervention methods, but a combined configuration is not used.

For this purpose, a linear one-track state space model and full vehicle model are prepared. The one-track model is used to design the required controllers. The full vehicle model is developed using CarMaker software and provides a virtual vehicle model representing actual vehicle dynamics to test the proposed configuration and designed controllers.

In order to test the effectiveness of the coordinated Steering and Braking (S+B) approach, test maneuvers are designed such that each maneuver provides a step or ramp input to one of the lateral position, angle, or angular rate errors.

An LQR is designed using the one-track model, then applied on the full vehicle model and tested using the step response maneuvers with (S+B) approach and only steering and only braking configurations. The results indicate that the (S+B) configuration is superior to only steering and only braking configurations in maintaining the longitudinal speed of the vehicle and keeping the vehicle in the lane, as well as having faster response and settling time.

Finally, an MPC is designed using the one-track model, applied on the full vehicle model, tested using the step response and ramp response maneuvers with only (S+B) approach, and compared with the LQR controller. The (S+B) configuration in company with MPC provides a more robust intervention than LQR.

The presented study fills a gap in the literature by proving the superior intervention performance of coordinated steering and braking configuration by taking advantage of the force potential of three wheels compared to common methods, which benefit from the force potential of only two wheels.

Further studies are planned using different controllers, road conditions,  $\mu$ -split cases, and vehicle configurations.



## 6. REFERENCES

- [1] NHTSA, "Early Estimates of Motor Vehicle Traffic Fatalities And Fatality Rate by Sub-Categories in 2021," May 2022. [Online]. Available: <https://crashstats.nhtsa.dot.gov/Api/Public/ViewPublication/813298>. [Accessed 09 November 2018].
- [2] J. C. Stutts and W. W. Hunter, "Driver inattention, driver distraction and traffic crashes," *ITE*, vol. 73, no. 7, pp. 34-45, 2003.
- [3] M. Dousti and E. Kutluay, "Binek Taşıtlara Yönelik Şerit Koruma Algoritmalarının Tartışılması Ve Yenilikçi Bir Algoritmanın Tanıtımı," in *OTEKON*, Bursa, 2016.
- [4] L. Palkovics and A. Fries, "Intelligent electronic systems in commercial vehicles for enhanced traffic safety," *Vehicle System Dynamic*, vol. 35, p. 227–289, 2001.
- [5] J. Pohl, W. Birk and A. Westervall, "A driver-distractionbased lane-keeping assistance system," *Proc IMechE, Part I: J Systems and Control Engineering*, vol. 221, p. 541–552, 2007.
- [6] L. Barr and W. Najm, "Crash problem characteristics for the intelligent vehicle initiative," Washington, DC., 2001.
- [7] J. Cicchino, "Effects of lane departure warning on police-reported crash rates," *Journal of Safety Research*, vol. 66, pp. 61-70, 2018.
- [8] Wikipedia, "Lane departure warning system," 2018. [Online]. Available: [https://en.wikipedia.org/wiki/Lane\\_departure\\_warning\\_system#cite\\_note-4](https://en.wikipedia.org/wiki/Lane_departure_warning_system#cite_note-4). [Accessed 12 12 2018].
- [9] EuroNCAP, "euroncap," 2018. [Online]. Available: <https://www.euroncap.com/en/vehicle-safety/the-rewards-explained/lane-support/>. [Accessed 01 01 2018].
- [10] K. BRAITMAN, A. MCCARTT, D. ZUBY and J. SINGER, "Volvo and Infiniti Drivers' Experiences With Select Crash Avoidance Technologies," *Traffic Injury Prevention*, vol. 11, no. 3, pp. 270-278, 2010.
- [11] M. Shimakage, S. Satoh, K. Uenuma and H. Mouri, "Design of lane-keeping control withsteering torque input," *Japan SAE*, vol. 23, pp. 317 - 323, 2002.
- [12] C. Edwards, J. Cooper and A. Ton, "Human Factors of Vehicle-Based Lane Departure Warning Systems," Minnesota Department of Transportation Research Services & Library, Minnesota, 2015.

- [13] A. Kullack, I. Ehrenpfordt, K. Lemmer and F. Eggert, "ReflektAS: lane departure prevention system based on behavioural control. Proc. IET Intelligent Transport Systems," *Intelligent Transport Systems*, vol. 2, no. 4, pp. 285-293, 2008.
- [14] V. D. Elzen, A. Nix, K. Michels, M. Wimmershof and A. Zlocki, "Control algorithm for hands-off lane centering on motorways," *20. Aachen Colloquium Automobile and Engine Technology*, 10-12 October 2011.
- [15] S. Ishida and J. E. Gayko, "Development, Evaluation and Introduction of a Lane Keeping Assistance System," *IEEE Intelligent Vehicles Symposium*, pp. 943 - 944, 14-17 June 2004.
- [16] A. Alleyne, "A Comparison of Alternative Intervention Strategies for Unintended Roadway Departure (URD) Control," *Vehicle System Dynamics: International Journal of Vehicle Mechanics and Mobility*, vol. 27, no. 3, pp. 157 - 186, 1997.
- [17] N. M. Enache, M. Netto, S. Mammar and B. Lusetti, "Driver steering assistance for lane departure avoidance," *Control Engineering Practice*, vol. 17, no. 6, pp. 642-651, 2009.
- [18] A. Gray, M. Ali, Y. Gao, J. K. Hedrick and F. Borrelli, "Integrated threat assessment and control design for roadway departure avoidance," in *15th International IEEE Conference on Intelligent Transportation Systems*, Anchorage, AK, USA, 2012.
- [19] Raksincharoensak, P., Nagai, M., Shino, M., "Lane keeping control strategy with direct yaw moment control input by considering dynamics of electric vehicle," *Vehicle System Dynamics*, vol. 44, no. 1, pp. 192 - 201, 2006.
- [20] J. F. Liu, J. H. Wu and Y. F. Su, "Development of an interactive lane keeping control system for vehicle," in *IEEE Vehicle Power and Propulsion Conference*, Arlington, TX, USA, 2007.
- [21] H. Kawazoe, T. Murakami, O. Sadano, K. Suda and H. Ono, "Development of a Lane-Keeping Support System," in *SAE Technical Paper*, Detroit, Michigan, 2001.
- [22] D. E. Williams, "Lane-keeping benefits of practical rear axle steer," *Vehicle System Dynamics*, vol. 52, no. 4, pp. 504 - 521, 2014.
- [23] D. E. Williams, "Improved Lane-Keeping with Rear Axle Steer," *SAE International*, pp. 137 - 146, 2015.
- [24] M. Oya and Q. Wang, "Adaptive Lane Keeping Controller for Four-Wheel-Steering Vehicles," Guangzhou, 2007.

- [25] P. Raksincharoensak, H. Mouri and M. Nagai, "Evaluation of four-wheel-steering system from the viewpoint of lane-keeping control," *International Journal of Automotive Technology*, vol. 5, no. 2, pp. 69 - 76, 2004.
- [26] Y. Hayakawa and T. Iwasaka, "Lane Departure Prevention Apparatus and Method". United States Patent US 2007/0255474 A1, 2007.
- [27] M. Lee, K. Hwang and I.-S. Suh, "Independent and Integrated Torque Control of 4-Wheel Drive Electric Vehicle for Automated Driving," *EVS28 International Electric Vehicle Symposium and Exhibition*, 3-6 May 2015.
- [28] Z. Liang, Y. Wang and G. Chen, "Control for four-wheel independently driven electric vehicles to improve steering performance using  $H_{\infty}$  and Moore–Penrose theory," *Proceedings of the Institution of Mechanical Engineers, Part D: Journal of Automobile Engineering*, vol. 233, no. 6, p. 1466–1479, 2019.
- [29] I. J. Reagan, D. G. Kidd and J. B. Cicchino, "Driver Acceptance of Adaptive Cruise Control and Active Lane Keeping in Five Production Vehicles," *Proceedings of the Human Factors and Ergonomics Society Annual Meeting*, vol. 61, no. 1, pp. 1949 - 1953, 2017.
- [30] Bedner E., Chen H., "A Supervisory Control to Manage Brakes and Four-Wheel-Steer Systems," in *SAE World Congress*, Detroit, 2004.
- [31] G. Palmieri, . M. Baric, F. Borrelli and L. Glielmo, "A Robust Lateral Vehicle Dynamics Control," *10th International Symposium on Advanced Vehicle Control*, 22 - 26 August 2010.
- [32] K. Gardels, "Automatic Car Controls for Electronic Highways," General Motors Corporation Research Laboratories, Warren, Michigan, 1960.
- [33] K. Cardew, "The Automatic Steering of Vehicles - An Experimental System Fitted to a DS 19 Citroen car," Road Research Laboratory, Crowthorne, Berkshire, 1970.
- [34] R. Fenton, G. MELOCIK and K. OLSON, "On the Steering of Automated Vehicles: Theory and Experiment," *IEEE Transactions on Automatic Control*, vol. 21, no. 3, pp. 306 - 315, 1976.
- [35] A. Alleyne, "A Comparison of Alternative Intervention Strategies for Unintended Roadway Departure (URD) Control," *Vehicle System Dynamics*, vol. 27, pp. 157-186, 1997.
- [36] S. Mammar, S. Chaib and M. S. Netto, "Hinfinity, Adaptive, PID and fuzzy control: a comparison of controllers for vehicle lane keeping," *IEEE Intelligent Vehicles Symposium*, pp. 139 - 144, 14 - 17 June 2004.

- [37] V. Cerone and D. Regruto, "Robust Performance Controller Design for Vehicle Lane Keeping," Cambridge, 2003.
- [38] V. Cerone and D. Regruto, "Vehicle lateral controller design exploiting properties of SITO systems," *IEEE Proceedings of the American Control Conference*, pp. 4365 - 4370, 4 - 6 June 2003.
- [39] R. Fenton and I. Selim, "On the Optimal Design of an Automotive Lateral Controller," *IEEE Transactions on Vehicular Technology*, vol. 37, no. 2, pp. 108 - 113, 1988.
- [40] P. Freeman, M. Jensen, J. Wagner and K. Alexander, "A Comparison of Multiple Control Strategies for Vehicle Run-Off-Road and Return," *IEEE Transactions on Vehicular Technology*, vol. 64, no. 3, pp. 901-911, 2015.
- [41] C. Bian, G. Yin, N. Zhang and L. Xu, "Takagi-Sugeno Fuzzy Model Predictive Controller Design for Combining Lane Keeping and Speed Tracking of Four Wheels Steering and Four Wheels Drive Electric Vehicle," Chongqing, 2017.
- [42] J. Lee and H. J. Chang, "Analysis of explicit model predictive control for path-following control," *PLOS ONE*, vol. 13, no. 3, 2018.
- [43] V. Turri, A. Carvalho, H. E. Tseng, K. H. Johansson and F. Borrelli, Linear model predictive control for lane keeping and obstacle avoidance on low curvature roads, *IEEE Annual Conference on Intelligent Transportation Systems*, 2013, pp. 378-383.
- [44] Pacejka H., *Tire and Vehicle Dynamics*, Oxford: Butterworth-Heinemann: Elsevier, 2012.
- [45] T. Kiper, "Proje Mühendisleri için Karayolu Geometrik Standartları Esasları," Karayolları Genel Müdürlüğü, ANKARA, 1988.
- [46] Peng, H., Tomizuka, M., "Preview Control for Vehicle Lateral Guidance in Highway Automation," *Journal of Dynamic Systems, Measurement, and Control*, vol. 115, no. 4, pp. 679-686, 1993.
- [47] B. Anderson and J. Moore, *Optimal control: Linear quadratic methods*, Prentice-Hall, 1990.
- [48] F. Lewis, D. Vrabie and V. Syrmos, *Optimal Control*, Third ed., New Jersey: John Wiley & Sons, Inc., 2012.
- [49] A. Bryson and Y.-c. Ho, *Applied Optimal Control*, Washington: John Wiley & Sons, 1975.
- [50] D. G. Luenberger, *OPTIMIZATION BY VECTOR SPACE METHODS*, New York: Wiley-Interscience, 1969.

- [51] A. Bemporad, M. Morari and L. Ricker, *Model Predictive Control Simulink Library*, Mathworks, 2010.
- [52] L. Wang, *Model predictive control system design and implementation using MATLAB*, London: Springer Science & Business Media, 2009.
- [53] G. Welch and G. Bishop, "An Introduction to the Kalman Filter," *Proc of SIG-GRAPH Course*, vol. 8, no. 27599-23175, 2006.
- [54] A. Bemporad and P. Patrinos, "Simple and Certifiable Quadratic Programming Algorithms for Embedded Linear Model Predictive Control," Noordwijkerhout, 2012.
- [55] J. Ferreau, H. G. Bock and M. Diehl, "An Online Active Set Strategy to Overcome the Limitations of Explicit MPC," *International Journal of Robust and Nonlinear Control*, vol. 18, no. 8, pp. 816 - 830, 2008.
- [56] Y. Wang and S. Boyd, "Fast Model Predictive Control Using Online Optimization," *IEEE Transactions on Control Systems Technology*, vol. 18, no. 2, 2010.
- [57] Türkiye İstatistik Kurumu, "Karayolu Trafik Kaza İstatistikleri, 2016," TÜİK, 2017.
- [58] J. Ackermann, *Robust Control: Systems with Uncertain Physical Parameters*, London: Springer, 1993.
- [59] IIHS-HLDI, "Insurance Institute for highway Safety - Highway Loss Data Institute Status Report SPECIAL ISSUE: CRASH AVOIDANCE," 2012. [Online]. Available: <https://www.iihs.org/iihs/sr/statusreport/article/47/5/1>. [Accessed 12 12 2018].
- [60] M. Oya and Q. Wang, "Adaptive lane keeping controller for four-wheel-steering vehicles," Guangzhou, 2007.
- [61] Kutluay, E., *Development and Demonstration of a Validation Methodology for Vehicle Lateral Dynamics Simulation Models*, Darmstad: fzd.tu, 2012.

# APPENDICES

## Appendix 1 – LQR Design

### Matlab Code:

```
%% Vehicle Parameters
m=1670; Iz=2100; a=0.99; b=1.7; h=0.508; U=28; d=0.76; Kfru=50539*2; Krru=20972*2;
Ca_f=-61595*2; Ca_r=-52095*2; Cla=-52526*2; Clr=-50000*2;
Clag=1.38; epsi=0.015; Jw=2;
rw=0.3;
g=9.81;

N=0;
%% State Space Matrices
A=[0 1 0 0 0;
  0 0 1 0 0;
  0 0 (Ca_f+Ca_r)/(m*U) -(Ca_f+Ca_r)/m (a*Ca_f-b*Ca_r)/(m*U);
  0 0 0 0 1;
  0 0 (a*Ca_f-b*Ca_r)/(Iz*U) -(a*Ca_f-b*Ca_r)/Iz (a^2*Ca_f+b^2*Ca_r)/(Iz*U)];

%% Case II. Front Wheel Steer + Rear Braking
B=[0 0 ;
  0 0 ;
  -Ca_f/m 0 ;
  0 0 ;
  -a*Ca_f/Iz -d/rw/Iz];

Q = diag([0.1 1 1 100 100]);

R = diag([2 1e-4]);

%% Method - 1
AT = transpose(A);
BT = transpose(B);

[P,s,K] = care(A,B,Q,R)

%% Method - 2
syms P11 P12 P13 P14 P15 P21 P22 P23 P24 P25 P31 P32 P33 P34 P35 P41 P42 P43 P44 P45 P51 P52
P53 P54 P55;
P = [P11 0 0 0 0
      0 P22 0 0 0
      0 0 P33 0 0
      0 0 0 P44 0
      0 0 0 0 P55];

Riccati = P*A + AT*P - P*B*R^(-1)*BT*P + Q;

G = B*R^(-1)*B';

H = [A -G; -Q -A'];
% [U,T] = SCHUR(X) produces a quasitriangular Schur matrix T and
% a unitary matrix U so that X = U*T*U' and U'*U = EYE(SIZE(U)).
% X must be square.
[U1, S1] = schur(H);
```

```

% [US,TS] = ORDSCHUR(U,T,SELECT) reorders the Schur factorization
% X = U*T*U' of a matrix X so that a selected cluster of eigenvalues
% appears in the leading (upper left) diagonal blocks of the
% quasitriangular Schur matrix T, and the corresponding invariant
% subspace is spanned by the leading columns of U.
% 'lhp' left-half plane (real(E)<0)
[U,S] = ordschur(U1,S1,'lhp');

[m,n] = size(A);
P = U(m+1:end,1:n) * U(1:m,1:n)^-1;

K = transpose(B * R^(-1)) * P

%% Method - 3
X0 = eye(5);

[T X] = ode45(@(t,X)mRiccati(t, X, A, B, Q), [0 10], X0)

[m n] = size(X);
XX = mat2cell(X, ones(m,1), n);
fh_reshape = @(x)reshape(x,size(A));
XX = cellfun(fh_reshape,XX,'UniformOutput',false);
K = transpose(B * R^(-1)) * XX{length(XX)}

function dXdT = mRiccati(t, X, A, B, Q)
X = reshape(X, size(A)); %Convert from "n^2"-by-1 to "n"-by-"n"
dXdT = A.*X + X*A - X*B*B.*X + Q; %Determine derivative
dXdT = dXdT(:); %Convert from "n"-by-"n" to "n^2"-by-1

```

## Appendix 2 – MPC Design

### Plant Model

Since the MPC approach is based on the prediction of the future outputs of the plant, the state space model of the plant is required to generate the desired control signal that allows the system to track the desired trajectory. The steps explained in the MPC Toolbox of Matlab are followed to develop an MPC algorithm. All formulas and derivations in this section can be found in [51].

The system's discrete-time state space model is used, as shown in (17).

$$\begin{aligned}x_p(k+1) &= A_p x_p(k) + B_p u_p(k) \\y_p(k) &= C_p x_p(k) + D_p u_p(k)\end{aligned}\tag{17}$$

where  $A_p, B_p, C_p, D_p$  are the model matrices obtained by the System Identification,  $x_p$ , system states and  $u_p$ , input vectors. Since the model include the measured disturbance inputs, (17) is rearranged by separating the  $B_p$  matrix columns into  $B_{pu}$  that corresponds to manipulated inputs  $u(k)$  and  $B_{pv}$  that corresponds to measured disturbance inputs  $v(k)$ . The following form is obtained.

$$\begin{aligned}x_p(k+1) &= A_p x_p(k) + B_{pu} u_p(k) + B_{pv} v(k) \\y_p(k) &= C_p x_p(k) + D_p u_p(k)\end{aligned}\tag{18}$$

The augmented form of system states, input vectors, and system matrices are:

$$A = A_p; B = [B_{pu} \quad B_{pv}]; C = C_p; D = D_p.$$

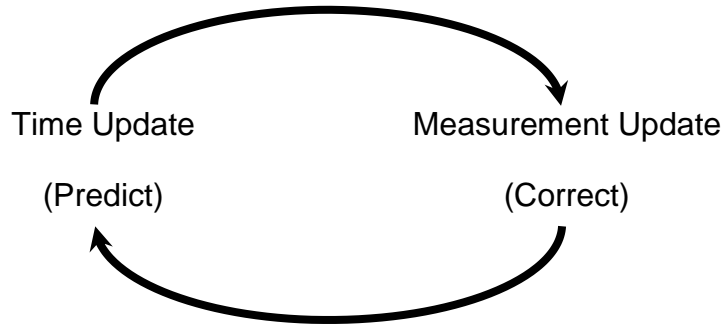
It is important to note that the controllability of the augmented model should be checked to achieve close-loop control performance, as mentioned in [52].

### Outputs Prediction

When system identification-based model derivation is performed, system states are not related to a physical variable and are not measurable. The first step is estimating these unknown states to predict future outputs based on the system model. For a successful state estimation, observability of the augmented system matrices ( $A, C$ ) is a pre-condition. Observability measures how well a system's internal states can be inferred from knowledge of its external outputs. The observability matrix must have a full degree, which is a necessary and sufficient condition.



Kalman filter is a popular state observer used in most control applications. It is a technique to estimate the unknown states based on a state space model, measured data, and noise covariance data. The basic diagram of the Kalman State Estimation is below:



Kalman State Estimation Cycle [53]

For a state space system with white noise process and measurement disturbances, state estimation process via the Kalman filter is as follows:

- Innovation variable  $e(k)$  is calculated based on the current measured plant output  $y_m(k)$  and the state estimate calculated from the previous step  $x_c(k|k-1)$  as:

$$e(k) = y_m(k) - Cx_c(k|k-1)$$

- A more accurate estimate of the state variable is calculated by using the newly measured information. This new state is:

$$x_c(k|k) = x_c(k|k-1) + Me(k)$$

- After optimum input is calculated, the future state estimate is computed as follows in order to use in the next control interval:

$$x_c(k+1|k) = Ax_c(k|k-1) + B_u u_{opt}(k) + B_v v(k) + Le(k)$$

where  $B_u$  and  $B_v$  are the columns of  $B$  corresponding to  $u$  and  $v$  vectors, respectively.

The second step above is referred to as the “Measurement Update” phase in the Kalman State Estimation Process, whereas the third step is called the “Time Update” phase. Here,  $M$  and  $L$  are the Kalman innovation, and estimator gain matrices are calculated using the Kalman function in Matlab. The inputs to the function are the observer model and noise covariance matrices that are calculated below:

$$Q = BB^T, R = DD^T, N = BD^T$$

The steady-state Kalman filter gain  $L$  and innovation gain  $M$  are calculated as:

$$L = PC^T R^{-1}, M = PC^T (CPC^T + R)^{-1}$$

To minimize the steady-state error covariance and the covariance matrix  $P$  is the solution to the Algebraic Riccati Equation:

$$AP + PA^T + BQB^T - PC^T R^{-1} CP = 0$$

More detailed information can be obtained from [53].

Prediction of future states at time  $k$  and within the optimization window  $N_p$  are calculated by:

$$\begin{aligned} x_c(k+1|k) &= Ax_c(k|k) + B_u u(k|k) + B_v v(k|k) \\ x_c(k+2|k) &= Ax_c(k+1|k) + B_u u(k+1|k) + B_v v(k+1|k) \\ &\vdots \\ x_c(k+N_p|k) &= Ax_c(k+N_p-1|k) + B_u u(k+N_p-1|k) + B_v v(k+N_p-1|k) \end{aligned}$$

And future predicted outputs at time  $k$  and within the optimization window  $N_p$  are:

$$\begin{aligned} y(k+1|k) &= Cx_c(k+1|k) + D_v v(k+1|k) \\ y(k+2|k) &= Cx_c(k+2|k) + D_v v(k+2|k) \\ &\vdots \\ y(k+N_p|k) &= Cx_c(k+N_p|k) + D_v v(k+N_p|k) \end{aligned}$$

Denote the columns of  $D$  matrix corresponding to manipulated inputs  $u$  and measured disturbances  $v$  in the overall output model as  $D_u$  and  $D_v$ , respectively. Although there is a  $D_u$  term, no direct feedthrough is assumed from  $u$  to  $y$  since the current plant output is required for both prediction and control. Therefore,  $D_u$  term is assumed as a zero matrix. On the other hand, specifically on the diesel engine model identified in this study,  $D_v$  term is found as a zero matrix; therefore,  $D$  term will not be used in the remaining calculations. However, it will be shown in equations. The calculations in the following sections are simplified by the introduction of  $\Delta u$  term as input change rate:

$$\Delta u(k) = u(k) - u(k-1)$$

After defining the vectors:

$$\begin{aligned} Y &= [y(k+1|k) \quad y(k+2|k) \quad y(k+3|k) \quad \cdots \quad y(k+N_p|k)]^T \\ \Delta U &= [\Delta u(k) \quad \Delta u(k+1) \quad \Delta u(k+2) \quad \cdots \quad \Delta u(k+N_c-1)]^T \\ V &= [v(k|k) \quad v(k+1|k) \quad v(k+2|k) \quad \cdots \quad v(k+N_p|k)]^T \end{aligned}$$

Moreover, putting together the predicted state equations, the output vector is given by:

$$Y = S_x x_c(k|k) + S_{u1} u(k-1) + S_u \Delta U + H_v V \quad (19)$$

where

$$\begin{aligned}
S_x &= \begin{bmatrix} CA \\ CA^2 \\ \vdots \\ CA^{N_p} \end{bmatrix}; S_{u1} = \begin{bmatrix} CB_u \\ CB_u + CAB_u \\ \vdots \\ \sum_{h=0}^{N_p-1} CA^h B_u \end{bmatrix} \\
S_u &= \begin{bmatrix} CB_u & 0 & \cdots & 0 \\ CB_u + CAB_u & CB_u & \cdots & 0 \\ \vdots & \vdots & \vdots & \vdots \\ N_{p-1} & N_{p-2} & \cdots & N_{p-N_c} \\ \sum_{h=0}^{N_{p-1}} CA^h B_u & \sum_{h=0}^{N_{p-2}} CA^h B_u & \cdots & \sum_{h=0}^{N_{p-N_c}} CA^h B_u \end{bmatrix} \\
H_v &= \begin{bmatrix} CB_v & D_v & 0 & \cdots & 0 \\ CAB_v & & & \cdots & 0 \\ \vdots & \vdots & \vdots & \vdots & \vdots \\ CA^{N_p-1} B_v & CA^{N_p-2} B_v & CA^{N_p-3} B_v & \cdots & D_v \end{bmatrix}
\end{aligned}$$

### Optimization

The general purpose of the MPC control design is to obtain a predicted output that follows the desired trajectory within a prediction horizon. To find such a control input that provides the goal, generally a quadratic cost function ( $J_{MPC}$ ) and constraints are defined.

A general form of a QP is as follows:

$$\begin{aligned}
&\min_x \frac{1}{2} z^T \bar{H} z + \bar{f}^T z \\
&\text{subject to } A_{in} z \leq b_{in} \\
&\quad A_{eq} z = b_{eq}
\end{aligned} \tag{20}$$

Then, the Quadratic Optimization Problem (QP) is solved by well-known QP solvers [54].

### Cost Function

The general cost function used in MPC applications contains four cost functions that are namely output reference tracking cost ( $J_y$ ), manipulated variable reference tracking cost ( $J_u$ ), manipulated variable change cost ( $J_{\Delta u}$ ), and a slack variable cost ( $J_\epsilon$ ), which is used to quantify the soft constraint violations. Each cost function contains a weighting factor within itself for prioritization. The overall cost function is:

$$J(z) = J_y(z) + J_u(z) + J_{\Delta u}(z) + J_\epsilon(z)$$

In this study, manipulated variables do not need to track a reference value but should remain in the desired range during the control process. Instead of including  $J_{\Delta u}$  in the cost function, it is added to the constraint part of the optimization problem.

The detailed form of cost functions are given below:

$$J_y = (Y - Y_{ref})^T Q (Y - Y_{ref}) \quad (21)$$

$$J_{\Delta u} = \Delta U^T R \Delta U \quad (22)$$

$$J_\epsilon = \rho_\epsilon \epsilon^2 \quad (23)$$

where  $Y_{ref}$  is the desired trajectory vector,  $Q$  is the output reference tracking weighting value,  $R$  is the weight matrix to pay attention to the size of  $\Delta U$ , and  $\rho_\epsilon$  is the constraint violation penalty.

To form an optimization problem like (20), firstly, the cost function (21) is rearranged.

By substituting (19) into (21), the following equation is obtained:

$$\begin{aligned} J_u &= (S_u \Delta U + c_y)^T Q (S_u \Delta U + c_y) \\ &= \Delta U^T S_u^T Q S_u \Delta U + 2c_y^T Q S_u \Delta U + c_y^T Q c_y \\ &= \Delta U^T S_a \Delta U + 2c_y^T Q S_u \Delta U + c_y^T Q c_y \end{aligned} \quad (24)$$

where

$$\begin{aligned} c_y &= S_x x_c(k|k) + S_{u1} u(k-1) + H_v V - Y_{ref} \\ S_a &= S_u^T Q S_u \end{aligned}$$

Due to  $c_y$  term depending only on the prediction state, previous step control input, measured disturbances, and output reference values, it does not affect the solution of the optimization problem; hence  $c_y^T Q c_y$  part is ignored in the cost function. By putting together all cost function terms together, we obtain

$$\begin{aligned} J &= \Delta U^T S_a \Delta U + 2c_y^T Q S_u \Delta U + \Delta U^T R \Delta U + \rho_\epsilon \epsilon^2 \\ &= \Delta U^T \underbrace{(S_a + R)}_H \Delta U + \underbrace{2c_y^T Q S_u}_{f^T} \Delta U + \rho_\epsilon \epsilon^2 \end{aligned} \quad (25)$$

Let the QP decision variable  $z$  be

$$z = [\Delta U \quad \epsilon]^T$$

Then we can rewrite the cost function as follows:

$$\begin{aligned} J &= \frac{1}{2} [\Delta U \quad \epsilon]^T \begin{bmatrix} 2H & 0 \\ 0 & 2\rho_\epsilon \end{bmatrix} \begin{bmatrix} \Delta U \\ \epsilon \end{bmatrix} + \begin{bmatrix} f^T \\ 0 \end{bmatrix} \begin{bmatrix} \Delta U \\ \epsilon \end{bmatrix} \\ &= \frac{1}{2} z^T \bar{H} z + \bar{f}^T z \end{aligned} \quad (26)$$

## Constraints

Another vital part of the MPC design is considering the constraints that are generally imposed on the outputs, inputs, and rate of change of the inputs.

The output constraints inequalities are written with the minimum and maximum output limits  $y_{min}$  and  $y_{max}$  and the constraint softness values  $v_{min}^y$  and  $v_{max}^y$  as follows:

$$\begin{aligned} \underbrace{\begin{bmatrix} y_{min}(k+1) \\ \vdots \\ y_{min}(k+N_p) \end{bmatrix}}_{Y_{min}} - \epsilon \underbrace{\begin{bmatrix} v_{min}^y(k+1) \\ \vdots \\ v_{min}^y(k+N_p) \end{bmatrix}}_{V_{min}^y} &\leq \underbrace{\begin{bmatrix} y(k+1|k) \\ \vdots \\ y(k+N_p|k) \end{bmatrix}}_Y \\ &\leq \underbrace{\begin{bmatrix} y_{max}(k+1) \\ \vdots \\ y_{max}(k+N_p) \end{bmatrix}}_{Y_{max}} + \epsilon \underbrace{\begin{bmatrix} v_{max}^y(k+1) \\ \vdots \\ v_{max}^y(k+N_p) \end{bmatrix}}_{V_{max}^y} \end{aligned}$$

The constraint softness and output limit values are assumed as constant during the prediction horizon  $N_p$ , i.e., we have

$$Y_{min} - \epsilon V_{min}^y \leq Y \leq Y_{max} + \epsilon V_{max}^y \quad (27)$$

Equation (27) can be transformed into the inequality matrices form as in (20):

$$\begin{aligned} -Y - \epsilon V_{min}^y &\leq -Y_{min} \\ Y - \epsilon V_{max}^y &\leq Y_{max} \end{aligned}$$

by putting  $Y$  as in (19),

$$\begin{aligned} -S_u \Delta U - \epsilon V_{min}^y &\leq -Y_{min} + S_x x_c(k|k) + S_{u1} u(k-1) + H_v V \\ S_u \Delta U - \epsilon V_{max}^y &\leq Y_{max} - S_x x_c(k|k) - S_{u1} u(k-1) - H_v V \end{aligned}$$

Then we can rewrite it as:

$$\underbrace{\begin{bmatrix} -S_u & -V_{min}^y \\ S_u & -V_{max}^y \end{bmatrix}}_{M_1} \underbrace{\begin{bmatrix} \Delta U \\ \epsilon \end{bmatrix}}_z \leq \underbrace{\begin{bmatrix} -Y_{min} \\ -Y_{max} \end{bmatrix}}_{N_{1c}} + \underbrace{\begin{bmatrix} S_x \\ -S_x \end{bmatrix}}_{N_{1x}} x_c(k|k) + \underbrace{\begin{bmatrix} S_{u1} \\ -S_{u1} \end{bmatrix}}_{N_{1u}} u(k-1) + \underbrace{\begin{bmatrix} H_v \\ -H_v \end{bmatrix}}_{N_{1v}} V$$

where

$$N_1 = N_{1c} + N_{1x} x_c(k|k) + N_{1u} u(k-1) + N_{1v} V;$$

so;

$$M_1 z \leq N_1 \quad (28)$$

The input constraints same procedure as in previous section is followed to get the input inequality constraints in QP format where  $u_{min}$  and  $u_{max}$  are the minimum and maximum input limits and  $v_{min}^u$  and  $v_{max}^u$  are the constraint softening values, i.e., the input constraints are represented as follows:

$$\begin{aligned} \underbrace{\begin{bmatrix} u_{min}(k) \\ \vdots \\ u_{min}(k + N_c - 1) \end{bmatrix}}_{U_{min}} - \epsilon \underbrace{\begin{bmatrix} v_{min}^u(k + 1) \\ \vdots \\ v_{min}^u(k + N_c - 1) \end{bmatrix}}_{V_{min}^u} &\leq \underbrace{\begin{bmatrix} u(k|k) \\ \vdots \\ u(k + N_c - 1|k) \end{bmatrix}}_U \\ &\leq \underbrace{\begin{bmatrix} u_{max}(k) \\ \vdots \\ u_{max}(k + N_c - 1) \end{bmatrix}}_{U_{max}} - \epsilon \underbrace{\begin{bmatrix} v_{max}^u(k + 1) \\ \vdots \\ v_{max}^u(k + N_c - 1) \end{bmatrix}}_{V_{max}^u} \end{aligned}$$

where

$$U_{min} - \epsilon V_{min}^u \leq U \leq U_{max} + \epsilon V_{max}^u \quad (29)$$

Then, the inequalities in (29) are rearranged, and the following inequalities are obtained:

$$\begin{aligned} -U - \epsilon V_{min}^u &\leq -U_{min} \\ U - \epsilon V_{max}^u &\leq U_{max} \end{aligned} \quad (30)$$

The next step is writing the  $U$  matrix for the optimization variable  $\Delta U$ . The relation between  $\Delta U$  and  $U$  is as follows:

$$\Delta U = \underbrace{\begin{bmatrix} I & 0 & 0 & \cdots & 0 & 0 \\ -I & I & 0 & \cdots & 0 & 0 \\ 0 & -I & I & \cdots & 0 & 0 \\ \vdots & \vdots & \vdots & \vdots & \vdots & \vdots \\ 0 & 0 & 0 & \cdots & -I & I \end{bmatrix}}_{T_1} U - \underbrace{\begin{bmatrix} I \\ 0 \\ 0 \\ \vdots \\ 0 \end{bmatrix}}_{T_2} u(k-1)$$

Then,  $U$  can be written as:

$$U = T_1^{-1} \Delta U + T_1^{-1} T_2 u(k-1)$$

After substituting  $U$  into (30), the input constraint matrices are transformed into the inequality matrices' form as in (19) by the following equations:

$$\begin{aligned} -T_1^{-1} \Delta U - \epsilon V_{min}^u &\leq -U_{min} + T_1^{-1} T_2 u(k-1) \\ T_1^{-1} \Delta U - \epsilon V_{max}^u &\leq U_{max} - T_1^{-1} T_2 u(k-1) \end{aligned}$$

Rewrite the inequality as below:

$$\underbrace{\begin{bmatrix} -T_1^{-1} & -V_{min}^u \\ T_1^{-1} & -V_{max}^u \end{bmatrix}}_{M_2} \underbrace{\begin{bmatrix} \Delta U \\ \epsilon \end{bmatrix}}_z \leq \underbrace{\begin{bmatrix} -U_{min} \\ U_{max} \end{bmatrix}}_{N_{2c}} + \underbrace{\begin{bmatrix} T_1^{-1} T_2 \\ -T_1^{-1} T_2 \end{bmatrix}}_{N_{2u}} u(k-1)$$

where  $N_2 = N_{2c} + N_{2u} u(k-1)$ , so:

$$M_2 z \leq N_2 \quad (31)$$

It is also possible to define the input rate constraints of change with the minimum and maximum  $\Delta u_{min}$  and  $\Delta u_{max}$  values. As in the previous steps,  $v_{min}^{\Delta u}$  and  $v_{max}^{\Delta u}$  are the constraint softening values and constraint inequalities can be written as follows:

$$\begin{aligned}
& \underbrace{\begin{bmatrix} \Delta u_{min}(k) \\ \vdots \\ \Delta u_{min}(k + N_c - 1) \end{bmatrix}}_{\Delta U_{min}} - \epsilon \underbrace{\begin{bmatrix} v_{min}^{\Delta u}(k + 1) \\ \vdots \\ v_{min}^{\Delta u}(k + N_c - 1) \end{bmatrix}}_{V_{min}^{\Delta u}} \leq \underbrace{\begin{bmatrix} \Delta u(k|k) \\ \vdots \\ \Delta u(k + N_c - 1|k) \end{bmatrix}}_{\Delta U} \\
& \leq \underbrace{\begin{bmatrix} \Delta u_{max}(k) \\ \vdots \\ \Delta u_{max}(k + N_c - 1) \end{bmatrix}}_{\Delta U_{max}} - \epsilon \underbrace{\begin{bmatrix} v_{max}^{\Delta u}(k + 1) \\ \vdots \\ v_{max}^{\Delta u}(k + N_c - 1) \end{bmatrix}}_{V_{max}^{\Delta u}}
\end{aligned}$$

where

$$\Delta U_{min} - \epsilon V_{min}^{\Delta u} \leq \Delta U \leq \Delta U_{max} + \epsilon V_{max}^{\Delta u} \quad (32)$$

Next, (32) rearranged as:

$$\begin{aligned}
& -\Delta U - \epsilon V_{min}^{\Delta u} \leq -\Delta U_{min} \\
& \Delta U - \epsilon V_{max}^{\Delta u} \leq \Delta U_{max} \\
& \underbrace{\begin{bmatrix} -I & -V_{min}^{\Delta u} \\ I & -V_{max}^{\Delta u} \end{bmatrix}}_{M_3} \underbrace{\begin{bmatrix} \Delta U \\ \epsilon \end{bmatrix}}_z \leq \underbrace{\begin{bmatrix} -\Delta U_{min} \\ \Delta U_{max} \end{bmatrix}}_{N_{2c}}
\end{aligned}$$

$$M_3 z \leq N_3 \quad (33)$$

As the last step, an extra inequality constraint is added to keep the slack variable  $\epsilon$  higher than 0:

$$\underbrace{\begin{bmatrix} 0 & -1 \end{bmatrix}}_{M_4} \underbrace{\begin{bmatrix} \Delta U \\ \epsilon \end{bmatrix}}_z \leq \underbrace{0}_{N_4}$$

$$M_4 z \leq N_4 \quad (34)$$

Then, all inequality constraints (28), (30), (33), and (34) are put together to obtain overall inequality matrices  $A_{in}$  and  $B_{in}$ :

$$\begin{aligned}
A_{in} &= [M_1 \quad M_2 \quad M_3 \quad M_4]^T \\
B_{in} &= [N_1 \quad N_2 \quad N_3 \quad N_4]^T
\end{aligned}$$

In summary, all constraints are arranged in the form of (20) so that the QP solver can be used.

### ***Quadratic Problem Solver***

For solving a QP (20), there are commonly used methods in the literature, namely Active Set Methods [55] and Interior Point Methods [56]. The QP solution method is not explained in this study. Matlab “*mpcqp solver*” function calculates the optimum  $z$  variable in each time step. The first element of  $z$  corresponds to rate of change of inputs in the first prediction step  $\Delta u(k|k)$ . Then, the optimum control signal  $u(k|k)$  that is applied to the system is obtained by adding the  $z(1)$  to previous control input as follows:

$$u(k|k) = u(k - 1) + z(1)$$

where  $z(1) = \Delta u(k|k)$ .



## Matlab Code:

1 – Prepare offline matrices:

In the beginning, the user-defined model parameters, disturbance parameters, input, input change, output constraints, controller sample time, prediction and control horizons, and cost function weightings are defined.

```
load('Vehicle_Parameters.mat');

mpcModel.PH = 50; % prediction horizon
mpcModel.CH = 10; % Control Horizon

mpcModel.plantModel = ss(Ap, [Bp, Fp], Cp, 0);
mpcModel.Ts = 0.01;

% manipulated variable interval, "The values presented here are examples and not real values for design"
mpcModel.uLowLimit = -0.5; % u1 minimum allowable steering angle (0.2 rad) u2 minimum road
disturbance (no limit for 1/rho)
mpcModel.uHighLimit = 0.5;
mpcModel.uMinECR = 0;
mpcModel.uMaxECR = 0;

% manipulated variable rate interval
mpcModel.uRateLowLimit = -1;
mpcModel.uRateHighLimit = 1;
mpcModel.uRateMinECR = 0;
mpcModel.uRateMaxECR = 0;

% control interval
mpcModel.yLowLimit = [-1.8;-3];
mpcModel.yHighLimit = [1.8;3];
mpcModel.yMinECR = [1;1];
mpcModel.yMaxECR = [1;1];

mpcModel.Q1 = 0.1;
mpcModel.Q2 = 10;
mpcModel.Q3 = 1;
mpcModel.Q4 = 100;
mpcModel.R = 2;
mpcModel.ro_epsilon = 100000;

%output disturbance matrices
mpcModel.outputDistModel.A_od = [];
mpcModel.outputDistModel.B_od = [];
mpcModel.outputDistModel.C_od = [];
mpcModel.outputDistModel.D_od = [];

%meas noise matrices
mpcModel.measurementNoiseModel.A_n = [];
mpcModel.measurementNoiseModel.B_n = [];
mpcModel.measurementNoiseModel.C_n = [];
mpcModel.measurementNoiseModel.D_n = [];

% Steering Control
OfflineCalcMatrices_m = calculateOfflineMatrices_mrtz(mpcModel);
```

## 2 – Offline Matrices Calculation:

All matrices, mentioned in previous part, are calculated with the calculateOfflineMatrices function given below. This function is called from the above m-file before the simulation is started.

```
function OfflineCalcMatrices = calculateOfflineMatrices(mpcModel)
```

```
Ts = mpcModel.Ts;
PH = mpcModel.PH; % prediction horizon
CH = mpcModel.CH; %Control Horizon
% manipulated variable interval
uLowLimit = mpcModel.uLowLimit;
uHighLimit = mpcModel.uHighLimit;
uMinECR = mpcModel.uMinECR;
uMaxECR = mpcModel.uMaxECR;

% manipulated variable rate interval
uRateLowLimit = mpcModel.uRateLowLimit;
uRateHighLimit = mpcModel.uRateHighLimit;
uRateMinECR = mpcModel.uRateMinECR;
uRateMaxECR = mpcModel.uRateMaxECR;

% control interval
yLowLimit = mpcModel.yLowLimit;
yHighLimit = mpcModel.yHighLimit;
yMinECR = mpcModel.yMinECR;
yMaxECR = mpcModel.yMaxECR;

Q1 = mpcModel.Q1;
Q2 = mpcModel.Q2;
Q3 = mpcModel.Q3;
Q4 = mpcModel.Q4;
R = mpcModel.R;
ro_epsilon = mpcModel.ro_epsilon;

OfflineCalcMatrices.Ts = Ts;
OfflineCalcMatrices.PH = PH;
OfflineCalcMatrices.CH = CH;
OfflineCalcMatrices.ro_epsilon = ro_epsilon;

%resample identified plant model
plantModel_resamp = c2d(mpcModel.plantModel,Ts);

plantModel_withoutDelay = absorbDelay(plantModel_resamp);

Ap=plantModel_withoutDelay.A;
Bp=plantModel_withoutDelay.B;
Cp=plantModel_withoutDelay.C;
Dp=plantModel_withoutDelay.D;

Bp_u = Bp(:,1); %manipulated variables
Bp_v = Bp(:,2); %measured disturbances !!

%output disturbance matrices
```

```

A_od = mpcModel.outputDistModel.A_od;
B_od = mpcModel.outputDistModel.B_od;
C_od = mpcModel.outputDistModel.C_od;
D_od = mpcModel.outputDistModel.D_od;

```

```

% meas noise matrices

```

```

A_n = mpcModel.measurementNoiseModel.A_n;
B_n = mpcModel.measurementNoiseModel.B_n;
C_n = mpcModel.measurementNoiseModel.C_n;
D_n = mpcModel.measurementNoiseModel.D_n;

```

```

% State Observer

```

```

[m1,n1]=size(Ap);
[m2,n2]=size(A_od);
A=eye(m1+m2,n1+n2);
A(1:m1,1:n1)=Ap;
A(m1+1:end,n1+1:end)=A_od;

```

```

[m1,n1]=size(Bp_u);
[m2,n2]=size(Bp_v);
[m3,n3]=size(B_od);
[m4,n4]=size(D_n);

```

```

B=zeros(m1+m3,n1+n2+n3+n4);
B(1:m1,1:n1)=Bp_u;
B(1:m1,n1+1:n1+n2)=Bp_v;
B(m1+1:end,n1+n2+1:n1+n2+n3)=B_od;

```

```

B_u = B(:,1); %for manipulated variables
B_v = B(:,2); %for measured disturbances !!

```

```

C = [Cp C_od];
D = [Dp D_od D_n];

```

```

OfflineCalcMatrices.A = A;
OfflineCalcMatrices.B_u = B_u;
OfflineCalcMatrices.B_v = B_v;
OfflineCalcMatrices.C = C;

```

```

% augmented plant with the output disturbance model

```

```

B_kal = eye(size(B,1));
D_kal = zeros(size(D,1),size(B,1));
Plant_Kalman = ss(A,B_kal,C,D_kal,Ts);

```

```

% State Estimation

```

```

Qn = B*B';
Rn = D*D';
Nn = B*D';
[~,L,~,M] = kalman(Plant_Kalman,Qn,Rn,Nn);

```

```

OfflineCalcMatrices.L = L;
OfflineCalcMatrices.M = M;

```

```

% Q matrix penalizes tracking error for performance.

```

```

Q_out = diag([Q1^2 Q2^2]);
% Q_out = diag([Q1^2 Q2^2 Q3^2 Q4^2]);
Q = Q_out;
for i=1:PH-1

```

```

    Q = blkdiag(Q,Q_out);
end

% R matrix penalizes MV rate of change for robustness.
R_u = R;
R = R_u;
for i=1:CH-1
    R = blkdiag(R,R_u);
end

%calculate matrices for J
[r1,c1] = size(A) ;
[r2,c2] = size(B_u) ;
[r3,c3] = size(B_v) ;
[r4,c4] = size(C) ;
Sx = ones(PH*r4,c1);
for i=1:PH
    j = i-1 ;
    Sx((j*r4+1):(i*r4),:) = C*(A^i) ;
end

Su_1 = zeros(PH*r4,c2);
for i=1:PH
    if i == 1
        Su_1(1:r4,:) = C*B_u ;
    else
        j = i-1 ;
        Su_1((j*r4+1):(i*r4),:) = Su_1(((j-1)*r4+1):(j*r4),:) + C*(A^j)*B_u ;
    end
end

Su = zeros(PH*r4,CH*c2) ;
for k =1:CH
    l= k-1 ;
    for i = 1:PH
        j = i-1 ;
        if(k>i)
            Su((j*r4+1):(i*r4),(l*c2+1):(k*c2)) = 0 ;
        else
            if i-k == 0
                Su((j*r4+1):(i*r4),(l*c2+1):(k*c2)) = C*B_u ;
            else
                Su((j*r4+1):(i*r4),(l*c2+1):(k*c2)) = Su(((j-1)*r4+1):(j*r4),(l*c2+1):(k*c2)) + C*(A^(i-k))*B_u ;
            end
        end
    end
end

Hv = zeros(r4*PH,c3*PH) ;
for k =1:PH
    l= k-1 ;
    for i = 1:PH
        j = i-1 ;
        if(k>i)
            Hv((j*r4+1):(i*r4),(l*c3+1):(k*c3)) = 0 ;
        else
            Hv((j*r4+1):(i*r4),(l*c3+1):(k*c3)) = C*(A^(i-k))*B_v ;
        end
    end
end

```

```

    end
  end
end

```

```

%matrices to convert U to deltaU

```

```

T1_ini = eye(c2,c2);
T1 = zeros(c2*CH,c2*CH) ;
for k =1:CH %column
    l= k-1 ;
    for i = 1:CH %row
        j = i-1 ;
        if(k==i)
            T1((j*c2+1):(i*c2),(l*c2+1):(k*c2)) = T1_ini ;
        elseif (i-k==1)
            T1((j*c2+1):(i*c2),(l*c2+1):(k*c2)) = -T1_ini;
        end
    end
end
end

```

```

T2 = zeros(c2*CH,c2);
T2(1:c2,1:c2) = eye(c2,c2);

```

```

%calculate matrices for J_deltaU

```

```

Hu = R;

```

```

%calculate matrices for Jy

```

```

Sa = Su'*Q*Su;
Hy = Sa;

```

```

Sb = 2*Su'*Q';
gy_1 = Sb*Su_1; %multiplied by u(-1)
gy_2 = Sb*Sx;
gy_3 = Sb*Hv;
gy_4 = -1*Sb;

```

```

%matrices for QP

```

```

H = 2*(Hu + Hy);
OfflineCalcMatrices.H = H;

```

```

OfflineCalcMatrices.g1 = gy_1; %multiplied part by u(-1)
OfflineCalcMatrices.g2 = gy_2; %multiplied part by x(0)
OfflineCalcMatrices.g3 = gy_3; %multiplied part by v
OfflineCalcMatrices.g4 = gy_4; %multiplied part by W

```

```

%Calculate matrices for inequality constraints

```

```

%matrices for input constraints

```

```

Vmin_U = repmat(uMinECR,CH,1);
Vmax_U = repmat(uMaxECR,CH,1);
Umin = repmat(uLowLimit,CH,1);
Umax = repmat(uHighLimit,CH,1);

```

```

M1 = [-1*(inv(T1)) -1*Vmin_U; inv(T1) -1*Vmax_U];
N1_c = [-1*Umin;Umax]; %%constant part
N1_u = [inv(T1)*T2;-1*(inv(T1)*T2)]; % multiplied by u(-1)

```

```

%matrices for input rate constraints
Vmin_deltaU = repmat(uRateMinECR,CH,1);
Vmax_deltaU = repmat(uRateMaxECR,CH,1);
deltaUmin = repmat(uRateLowLimit,CH,1);
deltaUmax = repmat(uRateHighLimit,CH,1);

M2 = [-1*eye(c2*CH) -1*Vmin_deltaU; eye(c2*CH) -1*Vmax_deltaU];
N2 = [-1*deltaUmin;deltaUmax];

%matrices for output constraints
Vmin_y = repmat(yMinECR,PH,1);
Vmax_y = repmat(yMaxECR,PH,1);
Ymin = repmat(yLowLimit,PH,1);
Ymax = repmat(yHighLimit,PH,1);

M3 = [-1*Su -1*Vmin_y; Su -1*Vmax_y];

N3_c = [-1*Ymin; Ymax]; %constant part
N3_x = [Sx; -1*Sx]; % multiplied by xp
N3_u = [Su_1; -1*Su_1]; % multiplied by u(-1)
N3_v = [Hv; -1*Hv]; % multiplied by v

%matrices for slack variable constraint
M4 = [zeros(1,c2*CH) -1];
N4 = 0;

OfflineCalcMatrices.M1 = M1;
OfflineCalcMatrices.M2 = M2;
OfflineCalcMatrices.M3 = M3;
OfflineCalcMatrices.M4 = M4;
OfflineCalcMatrices.N1_c = N1_c;
OfflineCalcMatrices.N1_u = N1_u;
OfflineCalcMatrices.N2 = N2;
OfflineCalcMatrices.N3_c = N3_c;
OfflineCalcMatrices.N3_x = N3_x;
OfflineCalcMatrices.N3_u = N3_u;
OfflineCalcMatrices.N3_v = N3_v;
OfflineCalcMatrices.N4 = N4;

```

### 3 - Online Matrices Calculation:

Lastly, calculateOnlineMatrices function is called from the Simulink MPCBlock at each sample of the simulation to calculate optimum manipulated variables.

```

function [mv,x_est] = calculateOnlineMatrices_mrtz(y,yref,u_prev,x_est_prev,md)
%%get offline calculated matrices for current region

OfflineCalcMatrices_curr = evalin('base','OfflineCalcMatrices_m');
OfflineCalcMatrices_m = evalin('base','OfflineCalcMatrices_m');

PH = OfflineCalcMatrices_curr.PH;
CH = OfflineCalcMatrices_curr.CH;
ro_epsilon = OfflineCalcMatrices_curr.ro_epsilon;

```

```

L = OfflineCalcMatrices_curr.L;
M = OfflineCalcMatrices_curr.M;
A = OfflineCalcMatrices_curr.A;
B_u = OfflineCalcMatrices_curr.B_u;
B_v = OfflineCalcMatrices_curr.B_v;
C = OfflineCalcMatrices_curr.C;
H = OfflineCalcMatrices_curr.H;
g1 = OfflineCalcMatrices_curr.g1; %multiplied part by u(-1)
g2 = OfflineCalcMatrices_curr.g2; %multiplied part by x(0)
g3 = OfflineCalcMatrices_curr.g3; %multiplied part by v
g4 = OfflineCalcMatrices_curr.g4; %multiplied part by W
M1 = OfflineCalcMatrices_curr.M1;
M2 = OfflineCalcMatrices_curr.M2;
M3 = OfflineCalcMatrices_curr.M3;
M4 = OfflineCalcMatrices_curr.M4;
N1_c = OfflineCalcMatrices_curr.N1_c;
N1_u = OfflineCalcMatrices_curr.N1_u;
N2 = OfflineCalcMatrices_curr.N2;
N3_c = OfflineCalcMatrices_curr.N3_c;
N3_x = OfflineCalcMatrices_curr.N3_x;
N3_u = OfflineCalcMatrices_curr.N3_u;
N3_v = OfflineCalcMatrices_curr.N3_v;
N4 = OfflineCalcMatrices_curr.N4;

%estimate state x
y_est = C*x_est_prev;
e = y - y_est;
xp = x_est_prev + M*e;

W = repmat(yref,PH,1);

md_aug = repmat(md,PH,1);
g = g1*u_prev + g2*x_est_prev + g3*md_aug + g4*W;
fq = g;

%augment cost function with slack variable
[r_H,c_H] = size(H);
Hbar = [H zeros(r_H,1);zeros(1,c_H) 2*ro_epsilon];
fbar = [fq;0];

%matrices for ineq constraints
N1 = N1_c + N1_u*u_prev;
N3 = N3_c + N3_x*xp + N3_u*u_prev + N3_v*md_aug;

M_in = [M1;M2;M3;M4];
N_in = [N1;N2;N3;N4];

[L_i,p_i] = chol(Hbar,'lower');
Lin_v = L_i\eye(size(Hbar,1));
A_in = -1*M_in;
B_in = -1*N_in;
A_eq = [];
B_eq = zeros(0,1);
opt = mpcqpsolverOptions;
iA0 = false(size(B_in));
[zbar_opt,status] = mpcqpsolver(Lin_v,fbar,A_in,B_in,A_eq,B_eq,iA0,opt);
% U_opt = quadprog(Hbar,fbar,A_in,B_in,A_eq,B_eq);

```

```

% U_opt = quadprog(H,fq);
% U_opt = quadprog(Hbar,fbar);

[r1,c1] = size(B_u);
if isempty(zbar_opt)
    zbar_opt = [zeros(c1*CH,1) 0];
end

% optimal move
mv = u_prev + zbar_opt(1:c1,1);

x_est = estimateStates(y,x_est_prev,md,mv,OfflineCalcMatrices_m);
end

```

#### 4 - State estimation

function called from calculateOnlineMatrices function is:

```
function x_est = estimateStates(y,x_est0,md,mv,OfflineCalcMatrices)
```

```

L = OfflineCalcMatrices.L;
A = OfflineCalcMatrices.A;
B_u = OfflineCalcMatrices.B_u;
B_v = OfflineCalcMatrices.B_v;
C = OfflineCalcMatrices.C;

%estimate state x
y_est = C*x_est0;
e = y - y_est;

x_est = A*x_est0 + B_u*mv + B_v*md + L*e;
end

```